An analysis of the variability of $\delta^{13}C$ in macroalgae from the Gulf of California

Roberto Velázquez-Ochoa[a], María Julia Ochoa-Izaguirre[b], Martín F. Soto-Jiménez[c*]

[a]Posgrado en Ciencias del Mar y Limnología, Universidad Nacional Autónoma de México, Unidad Académica Mazatlán, Mazatlán, Sinaloa 82040, México

[b]Facultad de Ciencias del Mar, Universidad Autónoma de Sinaloa. Paseo Claussen s/n, Mazatlán, Sinaloa 82000, México

[c]Unidad Académica Mazatlán, Instituto de Ciencias del Mar y Limnología, Universidad Nacional Autónoma de México (UAM-ICMyL-UNAM), Mazatlán Sinaloa, 82040, México.

Correspondent author:

Telephone number: +52 (669) 9852845 to 48.

Fax number: +52 (669) 9826133

E-mail: martin@ola.icmyl.unam.mx

Abstract

The isotopic composition of carbon in macroalgae ($\delta^{13}C$) is highly variable, and its prediction is very complex concerning terrestrial plants. To contribute to the knowledge about the variations and determinants of $\delta^{13}C$-macroalgal, we analyzed a large stock of specimens that vary in taxa and morphology and that inhabit shallow marine habitats in the Gulf of California (GC) featured by distinctive environmental conditions. A large $\delta^{13}C$ variability (-34.6‰ to -2.2‰) was observed, mainly explained by the life form (taxonomy, morphology, and structural organization), and modulated by the interaction between habitat features and environmental conditions. The intertidal zone specimens had fewer negative $\delta^{13}C$ values than in the subtidal zone. Except for pH, environmental conditions of the seawater do not contribute to the $\delta^{13}C$ variability. Specimens of the same taxa showed $\delta^{13}C$ similar patterns, to increase or decrease, with latitude (21°-30°N). $\delta^{13}C$-macroalgal provides information on the inorganic carbon source used for photosynthesis (CO_2 diffusive entry vs HCO_3^- active uptake). Most species showed a $\delta^{13}C$ belong into a range that indicates a mix of CO_2 and HCO_3^- uptake (strategy 2: $-10<\delta^{13}C>-30$‰); however, the HCO_3^- uptake by active transport (strategy 1: $\delta^{13}C>-10$‰) is also widespread among GC macroalgae. Ochrophyta presented a high number of species with $\delta^{13}C>-10$‰. Few species belonging to Rhodophyta relied on CO_2 diffusive entry (strategy 3: $\delta^{13}C<-30$‰) exclusively. Few calcifying macroalgae species using HCO_3^- and diffusive CO_2 (strategy 4) were also collected, such as *Amphiroa* and *Jania*. The $\delta^{13}C$ values of macroalgae integrate the isotope discrimination during carbon assimilation and, to a lesser extent, during the respiration across its lifecycle, thus providing useful information on the physiological and environmental status of macroalgae.

Keywords: $\delta^{13}C$-macroalgal, carbon-concentrating mechanisms, CO_2 diffusive proxy

1. Introduction

Macroalgae show a wide diversity of thallus morphologies (e.g., filamentous, articulated, flattened), structural organization (e.g., surface area/volume ratio), and various photosynthetic pigments (e.g., Chlorophyll *a*, *b*, phycocyanin) (Lobban and Harrison, 1994). Based on these features, macroalgae can be classified into only three Phyla, according to the predominant pigment contents in the thallus, or into dozens of groups considering the interaction of morphologies and photosynthetic pigments (Littler and Littler, 1980; Littler & Arnold, 1982; Balata et al., 2011). For example, the mixture of chlorophyll (*a*, *b*) and carotenoids is dominant in Chlorophyta; chlorophyll (*a*, *c*) and fucoxanthin carotenoid is dominant in Ocrophyta, while Rhodophyta contains chlorophyll (*a*, *d*), carotenoid, and a mixture of phycobilin (e.g., phycocyanin, phycoerythrina, allophycocyanin) (Bold and Wynne, 1978; Masojidek et al., 2004; Gateau et al., 2017). Both traits work as an excellent approximation to explain the fundamentals of metabolism, growth, zonation, and colonization (Littler and Littler, 1980; Littler and Arnold, 1982; Nielsen and Sand-Jensen, 1990; Vásquez-Elizondo and Enríquez, 2017).

The thickness of the thallus as a propriety of morphology influences the diffusion boundary layer on surface of the macroalgal, where they carry out the absorption of essential ions and dissolved gases (Hurd, 2000; San-Ford and Crawford, 2000). In marine environments, where pH~8.1±1, HCO_3^- accounts for 98% of the total DIC due to the low diffusion rate of CO_2 in seawater that results in a high HCO_3^-:CO_2 ratio (150:1) (Sand-Jensen and Gordon, 1984). The limitations to growth imposed by low CO_2 concentrations in seawater are compensated by carbon concentration mechanisms (CCMs) in most macroalgae that increase the internal inorganic carbon concentration near the site of RuBisCo activity (Giordano et al., 2005). Therefore, the absorption of HCO_3^- by most macroalgae is the main source of inorganic carbon for photosynthesis, but some species depend exclusively on the use of dissolved CO_2 that enters cells by diffusion (Maberly et al., 1992; Beardall and Giordano,

2002; Raven et al., 2002a, b; Giordano et al., 2005). Hence, macroalgal species with productivity limited by lacking CCM's (have low plasticity for carbon inorganic forms uptake) seems to be restricted to subtidal habitats and composed mainly by red macroalgae (but without a morphological patron apparent) (Cornwall et al., 2015, Kübler and Dungeon, 2015). The rest of the macroalgae with CCM occupies from the intertidal to the deep subtidal.

Nevertheless, marine ecosystems have many environmental factors, including habitat features and environmental conditions in seawater that modify the main macroalgae photosynthesis drivers as light (Anthony et al., 2004; Johansson and Snoeijs, 2014), DIC (Zeebe and Wolf-Gladrow, 2001; Brodeur et al., 2019), and inorganic nutrients (Teichberg et al., 2010; Ochoa-Izaguirre and Soto-Jiménez, 2015). These factors could generate negative consequences for their productivity, principally when they cause resources limitation. Each factor varies from habitat to habitat (e.g., local scale: from intertidal to subtidal and global scale: from temperate to tropical regions), and as in response to these environmental changes, macroalgae can modulate their photosynthetic mechanism (Lapointe and Duke, 1984; Dudgeon et al., 1990; Kübler and Davison 1993, Young et al., 2005). The modulation, to increase their photosynthetic activity (up-and-down-regulation processes), implies a physiological acclimation enhancing the transport of DIC (CO_2, HCO_3^-) into the cell and its fixation rates (Madsen and Maberly, 2003; Klenell et al., 2004; Zou et al., 2004; Giordano et al., 2005; Enríquez and Rodriguez-Román, 2006; Rautemberger et al., 2015).

The $\delta^{13}C$ on the thallus of marine macrophytes is a proxy used to identify CO_2 or HCO_3^- source in photosynthesis and to infer the presence or absence of CCM's (Maberly et al., 1992; Raven et al., 2002a). Also, the $\delta^{13}C$ signal in the algal thallus can be used as an indicator of the physiological state of photosynthetic metabolism (Kim et al., 2014; Kübler and Dungeon, 2015). For example, $\delta^{13}C$ variability depends, in part, on the life forms as taxonomy, morphology, and structural organization (Mercado et al., 2009, Marconi et al., 2011, Lovelock et al., 2020), but also is modulated by the

interaction to environmental conditions (e.g., light, DIC, and nutrients) (Cornelisen et al., 2007; Dudley et al., 2010; Carvalho et al., 2010ab; Mackey et al., 2015; Rautenberger et al., 2015).

In this study, our objective was to investigate the contributions of life form, the changes in the habitat features, and environmental conditions to the $\delta^{13}C$ macroalgal variability in communities in the Gulf of California (GC). To reach our objective, we collected a large stock of macroalgae specimens of a diversity of species characterized by a variety of morphological and physiological properties. Besides high diversity, in terms of life forms, we selected various shallow marine habitats along a latitudinal gradient in the GC or the sample collection, characterized by unique and changing environmental factors. The GC features abundant and diverse macroalgae populations, which are acclimated and adapted to diverse habitats with environmental conditions, determining the light, DIC, and nutrients availability. The $\delta^{13}C$ signal from the thallus of macroalgae was also used to infer carbon uptake strategies in macroalgae communities in the GC in function of taxa and environmental factors (Maberly et al., 1992; Raven et al., 2002; Hepburn et al., 2011; Díaz-Pulido et al., 2016). Because the GC is a subtropical zone with high irradiance and specimens were collected in the intertidal and subtidal zone, we expect to find a high proportion of species with active uptake HCO_3^- ($\delta^{13}C$>-10‰). A third objective was to explore any geographical pattern in the $\delta^{13}C$ macroalgal along and between the GC bioregions. Previous studies have indicated changes in the $\delta^{13}C$ signal with latitude, mainly related to the light and temperature (Mercado et al., 2009; Marconi et al., 2011; Stepien, 2015; Hofmann and Heesch, 2018; Lovelock et al., 2020). Macroalgae as biomonitor constitute an efficient tool in monitoring programs in large geographical regions (Balata et al., 2011) and for environmental impact assessments (Ochoa-Izaguirre and Soto-Jiménez, 2015).

2. Materials and Methods

2.1. Gulf of California description

111 The Gulf of California is a subtropical, semi-enclosed sea of the Pacific coast of Mexico, with
112 exceptionally high productivity being the most important fishing regions for Mexico and one of the
113 most biologically diverse worldwide marine areas (Zeitzschel, 1969; Espinosa-Carreón and Valdez-
114 Holguín 2007; Lluch-Cota et al., 2007; Páez-Osuna et al., 2017). GC represents only 0.008% of the
115 area covered by the seas of the planet (265,894 km^2, 150 km wide, and 1000 km long covering >9
116 degrees latitude) but has a high physiographic diversity and is biologically mega-diverse with many
117 endemic species, including ~ 766 macrofauna species and/or sub-species where the major number
118 belong to Arthropoda (118 spp) and Mollusca (460) taxas (Brusca et al., 2005; Wilkinson et al.,
119 2009; Espinosa-Carreón and Escobedo-Urías, 2017) and 116 macroalgae species (Norris, 1975,
120 1985; Espinoza-Avalos, 1993).

121 Regionalization criteria of the GC include phytoplankton distribution (Gilbert and Allen, 1943),
122 topography (Rusnak et al., 1964) and depth (Álvarez-Borrego, 1983), oceanographic characteristics
123 (Roden and Emilson, 1979; Álvarez-Borrego, 1983; Marinone and Lavin 2003), biogeography
124 (Santamaría-del-Ángel et al., 1994), and bio-optical characteristics (Bastidas-Salamanca et al.,
125 2014). The topography is variable along with GC, includes submarine canyons, basins, and variable
126 continental platforms. Besides, GC presents complex hydrodynamic processes, including internal
127 waves, fronts, upwelling, vortices, mixing of tides. The gulf's coastline is divided into three shores:
128 extensive rocky shores, long sandy beaches, numerous scattered estuaries, coastal lagoons, and open
129 muddy bays tidal flats, and coastal wetlands (Lluch-Cota et al., 2007).

130 The Gulf of California is different in the north and the south, related to a wide range of
131 physicochemical factors. The surface currents seasonally change direction and flow to the southeast
132 with maximum intensity during the winter and to the northwest in summer (Roden (1958). The
133 northern part is very shallow (<200 m deep averaged), divided into Upper Gulf, northern Gulf, and

Grandes Islas. The surrounding desserts largely influence this region (Norris, 2010) shows marked seasonal changes in coastal seawater temperatures (Martínez-Díaz de León et al., 2006; Marinone, 2007). Tidal currents induce a significant cyclonic circulation through June to September and anticyclonic from November to April (Carrillo et al., 2002; Bray, 1988a; Velasco-Fuentes and Marinone, 1999; Martínez-Díaz-de-León, 2001). The southern part consists of a series of basins whose depths increase southwards (Fig. 1). The intertidal macroalgae in the southern region are subject to desiccation, mostly during summer. The water column's physicochemical characteristics are highly influenced by the contrasting climatic seasons in the GC, the dry season (nominally from November to May), and the rainy season (from June to October). Annual precipitation (1,080 mm y^{-1}) and evaporation (56 mm y^{-1}) rates registered during the past 40 years were 881±365 mm y^{-1} and 53±7 mm y^{-1}, respectively (CNA, 2012).

Previous macroalgae floristic studies of the GC, report around 669 species, including 116 endemic species (Norris, 1975; Espinoza-Avalos, 1993; Pedroche and Senties, 2003). Many endemic species currently have a wide distribution along the Pacific Ocean coast, but with GC origin (Dreckman, 2002; Aguilar-Rosas et al., 2014). Based on oceanographic characteristics (Roden and Groves, 1959) and in the endemic species distribution (Aguilar Rosas and Aguilar Rosas, 1993; Espinoza-Avalos, 1993), the GC can be classified into three phycofloristic zones: 1) the first zone located from the imaginary line connecting San Francisquito Bay, B.C. to Guaymas, Sonora, with 51 endemic species. 2) the second zone with an imaginary line from La Paz bay (B.C.S.) to Topolobampo (Sinaloa) with 41 endemic species. 3) the third zone is located with an imaginary line from Cabo San Lucas (B.C.S.) to Cabo Corrientes (Jalisco) with 10 endemic species. Besides, 14 endemic species are distributed throughout the GC (Espinoza-Ávalos, 1993). The macroalgal communities are subject to the changing environmental conditions in the diverse habitats in the GC

157 that delimits their zonation, which tolerates a series of anatomical and physiological adaptations to
158 water movement, temperature, sun exposure, and light intensities, low pCO2, desiccation (Espinoza-
159 Avalos 1993).

160 **2.1 Macroalgae sampling**

161 In this study, the GC coastline (21º-30°N latitude) was divided into six coastal sectors based on the
162 three phycofloristic zones along peninsular and continental GC coastlines (Fig. 1a). In each coastal
163 sector, selected ecosystems and representative habitats were sampled based on macroalgae
164 communities' presence and habitat characterization. Habitats were classified by substrate type (e.g.,
165 sandy-rock, rocky shore), hydrodynamic (slow to faster water flows), protection level (exposed or
166 protected sites), and immersion level (intertidal or subtidal) (Fig. 1b).

167 Based on the local environmental factors, macroalgae specimens (4-5) of the most representative
168 species were gathered by hand (free diving) during low tide. A total of 809 composite samples were
169 collected from marine habitats along both GC coastlines. The percentages of specimens collected for
170 the substrate type were sandy-rock 28% and rocky shores 72% based on the habitat features. Related
171 to the hydrodynamic, 30% of the specimens were collected in habitats with slow to moderate and
172 70% with moderate to fast water movement. Regarding the protection level, 57% were exposed
173 specimens, and 43% were protected. Finally, 56% were intertidal and 44% subtidal macroalgae
174 organisms concerning the emersion level. About half of the protected specimens were collected in
175 isolated rock pools, which was noted.

176 In 4-5 sites of each habitat, we measured *in situ* the salinity, temperature, and pH by using a
177 calibrated multiparameter sonde (Y.S.I. 6600V) and the habitat characteristics mentioned above
178 noted. Besides, composite water samples were collected for complementary analysis of nutrient,

alkalinity (and their chemical components), and δ^{13}C-DIC (data non-included). Briefly, the representative habitats were classified by pH levels in >9.0 “alkalinized”, 7.9-8.2 ‘typical’ and <7.9 “acidified”. Based on the temperature in colder <20ºC, typical 20-25ºC, and warmer >25ºC. 72% of the specimens were collected at typical pH values, 22% in alkalinized and 6% in acidified seawater. Regarding the temperature, about 55% of the specimens were collected at typical, 31% at warmer, and 14% at colder seawaters. Regarding salinity, most of the ecosystems showed typical values for seawater (35.4±0.91 ups, from 34.5 to 36.1 ups). In this study, the collection surveys were conducted during spring (March-April) and dry season (nominally from November to May) from 2009 to 2014. Only in few selected ecosystems located at C1 and C2 sectors, one sampling survey was conducted at the end of the rainy season (nominally from June to October in 2014). Thus, these ecosystems were possible to include habitat with a salinity range varying from estuarine (23.5±3.0 ups) to hypersaline (42.7±7.0 ups) values. These habitats were mainly isolated rockpools, and only a few were sites near tidal channels receiving freshwater discharges. About 95% of the specimens were collected at typical seawater salinity (34-36 ups) and only 1.5 and 3.5% in estuarine (<30 ups) and hypersaline (>37 ups) environments, respectively. Detailed information on the selected shallow marine ecosystems, habitat characterization, and environmental conditions is summarized in the inserted table in Fig. 1.

2.2 Macroalgae processing and analysis of the isotopic composition of carbon

The collected material was washed *in situ* with surface seawater to remove the visible epiphytic organisms, sediments, sand, and debris and then thoroughly rinsed with MilliQ water. The composite samples were double-packed in a plastic bag, labeled with the locality's name and collection date, placed in an ice-cooler box to be kept to 4ºC, and immediately transported to the laboratory UAS-Facimar in Mazatlán. In the field, sample aliquots were also preserved in 4% v/v formaldehyde

202 solution for taxonomic identification to the genus or species level (when possible). The following
203 GC macroalgal flora identification manuals were consulted: Dawson, 1944; 1954; 1956; 1961; 1962;
204 1963; Setchell and Gardner, 1920; 1924; Abbott and Hollenberg, 1976; Ochoa-Izaguirre et al., 2007;
205 Norris, 2010).

206 In the laboratory, macroalgae samples were immediately frozen at -30ºC until analysis. Then,
207 samples were freeze-dried at -38ºC and 40 mm Hg for 3 days, upon which they were ground to a
208 fine powder and exposed to HCl vapor for 4 h (acid-fuming) to remove carbonates and dried at 60ºC
209 for 6 h (Harris et al. 2001). Aliquots of ~5 mg were encapsulated in tin cups (5x9 mm) and stored in
210 sample trays until analysis. Macroalgae samples were sent to the Stable Isotope Facility (SIF) at the
211 University of California at Davis, CA, USA. Natural ^{13}C relative abundance relative to ^{12}C in
212 samples was determined with mass spectrometry, using a Carlo Erba elemental analyzer attached to
213 a Finnigan Delta S mass spectrometer equipped with a Europa Scientific stable isotope analyzer
214 (ANCA-NT 20-20) and a liquid/solid preparation unit (PDZ, Europa, Crewz, UK). Isotope ratios of
215 the samples were calculated using the equation δ (‰)=($R_{sample}/R_{standard}$-1)]x1000, where $R=^{13}C/^{12}C$.
216 The $R_{standard}$ is relative to the international V-PDB (Vienna PeeDee Belemnite) standard. During the
217 isotopic analysis, the SIF lab used different certified reference materials (e.g., IAEA-600, USGS-40,
218 USGS-41, USGS-42, USGS-43, USGS-61, USGS-64, and USGS-65) for the analytical control
219 quality. The analytical uncertainties reported for the SIF lab were 0.2‰ for $\delta^{13}C$
220 (https://stableisotopefacility.ucdavis.edu/13cand15n.html). We also included triplicate aliquots of
221 several specimens of the same species and condition, collected from one patch, or attached to the
222 same substrate, to assess the method error by sampling and processing procedural. The
223 methodological uncertainties were <0.4‰.

224 **2.3. Analysis of $\delta^{13}C$-macroalgal variability**

The variability of $\delta^{13}C$ values in macroalgae was analyzed in function of the taxonomy (phylum, genus, and species) and morpho-functional groups (e.g., thallus structure, growth form, branching pattern, and taxonomic affinities; Balata et al. 2011; Ochoa-Izaguirre and Soto-Jiménez, 2015). The carbon fixation strategies in the macroalgae communities of the GC were identify by $\delta^{13}C$ (Hepburn et al., 2011; Díaz-Pulido et al., 2016), in agreement with the Maberly et al. (1992) and Raven et al. (2002) thresholds. So, macroalgae were classified into four strategies for DIC uptake: 1) CCM-only by active uptake HCO_3^- ($\delta^{13}C$>-10‰), 2) CCM active uptake HCO_3^- and/or diffusive uptake CO_2 ($\delta^{13}C$<-11 to -30‰), 3) Non-CCM, CO_2 by diffusion only ($\delta^{13}C$<-30‰), 4) Calcifying with different carbon-use strategies related to different modes of calcification. The measured $\delta^{13}C$-macroalgal signals are integrative of the discrimination by photosynthesis ($\Delta^{13}C_p$) on the carbon source ($\delta^{13}C$-DIC in seawater), respiration ($\Delta^{13}C_r$), and probable CO_2 leak out inside the cell during the CCM process (Sharkey and Berry, 1985; Raven et al., 2005; Carvalho et al., 2009a,b).

To find a geographic pattern associated with the $\delta^{13}C$ signal of macroalgae in this study, macroalgae were grouped according to their characteristics morpho-functional proposed initially by Littler and Littler (1980) and modified by Balata et al. (2011). Not all morphofunctional groups and taxon were present in every site during each sampling survey, and the sample size in each group varied for taxa, location, and time.

A basic statistical analysis of $\delta^{13}C$ values in different macroalgae groups was applied to distribute and calculate the arithmetic mean, standard deviation, minimum and maximum. Because not all macroalgal species were present in sufficient numbers at different collection habitats, several macroalgal groups were not considered for statistical analysis. Regarding the life form, we compared among morphofunctional groups, taxon collected in the same habitat (within-subjects factor) by multivariate analysis of variance. When differences were noted, a Tukey-Kramer HSD (Honestly

248 Significant Difference) test was performed. Besides, variations of $\delta^{13}C$ macroalgal in specimens of
249 the same morpho-functional and taxon collected in different habitats were also investigated with a
250 Kruskal-Wallis test.

251 In this study, the relationships between $\delta^{13}C$ with each independent variable related to the inherent
252 macroalgae properties (morphology and taxon), biogeographical collection zone (GC coastline and
253 coastal sector), habitat features (substrate, hydrodynamic, protection, and emersion level) and
254 environmental conditions (temperature, pH, and salinity) were examined through simple and
255 multiple linear regression analyses. Excepting temperature, pH, and salinity, most of the independent
256 variables are categorical independent variables. However, these continue variables were also
257 categorized, such as previously was described. Analyses of simple linear regression were performed
258 to establish the relationships between $\delta^{13}C$-macroalgal with each environmental parameter analyzed
259 as possible driving factors (e.g., temperature, salinity, pH). Multiple linear regression analyses were
260 conducted to evaluate the combined effects of those independent variables (macroalgae properties,
261 biogeographical collection zone, habitat features, and environmental conditions) on the $\delta^{13}C$-
262 macroalgal. In the multivariable regression model, the dependent variable, $\delta^{13}C$-macroalgal, is
263 described as a linear function of the independent variables X_i, as follows: $\delta^{13}C\text{-macroalgal} = a +$
264 $b_1(X_1) + b_2(X_2) + \ldots + b_n(X_n)$ (1). Where a is regression constant (it is the value of intercept and its
265 value is zero); b_1, b_2, and b_n, are regression coefficients for each independent variable X_i. From each
266 one of the fitted regression models, we extracted the estimated regression coefficients for each of the
267 predictor variables (e.g., Bayesian Information Criterion (BIC), Akaike Information Criterion (AIC),
268 root-mean-square error (RMSE), Mallow's Cp criterion, F Ratio test, p-value for the test (Prob > F),
269 coefficients of determination (R^2) and the adjusted R^2 statistics) (SAS Institute Inc., 2018). All
270 regression coefficients were used as indicators of the quality of the regression (Draper and Smith,

1998; Burnham and Anderson, 2002). Kolmogorov-Smirnov normality test was applied for all variables, and all were normally distributed. Most of the $\delta^{13}C$ values in each group showed a normal distribution. For all statistical tests, a probability $P<0.05$ was used to determine statistical significance. The statistical analysis of the results was done using JMP 14.0 software (SAS Institute Inc.).

3. Results

3.1. Taxonomy and morpho-functional groups

Sampled specimens belong to three Phyla, 63 genera, and 167 species. The Phyla were identified as Chlorophyta (25%), Ochrophyta (22%), and Rhodophyta (53%). The most representative genus (and their species) were *Ulva* (*U. lactuca, U. lobata, U. flexuosa,* and *U. intestinalis*), *Codium* (*C. amplivesiculatum* and *C. simulans*), *Chaetomorpha* (*C. antenina*), *Padina* (*P. durvillaei*), *Dictyota* (*D. dichotoma*), *Colpomenia* (*C. tuberculata* and *C. sinuosa*), *Sargassum* (*S. sinicola* and *S. horridum*), *Amphiroa* (*Amphiroa* spp.), *Spyridia* spp, *Polysiphonia* spp., *Gymnogongrus* spp., *Gracilaria* (*G. vermiculophylla, G. pacifica* and *G. crispate*), *Hypnea* (*H. pannosa* and *H. johnstonii*) *Grateloupia* (*G. filicina* and *G. versicolor*), and *Laurencia* (*L. papillosa* and *L. pacifica*). An analysis of the biogeographical diversity among sectors evidenced that P3 (43 genera of 63, 68%) and C3 (63%) at north recorded the highest number of the genus, followed by C1 (38%) and P1 (29%) at the south, and P2 (27%) and C2 (22%). The same pattern was observed in the species richness, zones P3 (94 of 167 species, 56%) and C3 (52%) at the north, C1 (34%) and P1 (25%) at the south, and C2 and P2 (19-20%) at the center. In our study, the endemic species includes Chlorophyta *Codium amplivesiculatum*, Rhodophyta *Laurencia papillosa*, *Chondracanthus squarrulosa*, *Gracilaria spinigera,* and *Gracilaria subsecundata*, and Ochrophyta *Cutleria hancockii, Sargassum*

herphorizum, Sargassum johnstonii.

The morphofunctional groups identified were 21, of which the most common were C-tubular (6 spp., n=69; C-Blade-like (6 spp, n=55); C-Filamentous uniseriate (17 spp, n=49); C-Erect thallus (5 spp, n=33); O-Compressed with branched or divided thallus (19 spp., n=92); O-Thick leathery macrophytes (12 spp., n=104); O-Hollow with spherical or subspherical shape (4spp, n=87); R-Large-sized corticated (57 spp., n=225); R-Filamentous uniseriate and pluriseriate with erect thallus (9 spp., n=48); and R-Large-sized articulated corallines (6 spp, n=17). The diversity, in terms of presence/absence of the morphofunctional groups, varied among coastline sectors, higher in C3 (16 of 21, 76%) and P3 (71%) at the north, followed by C1 (57%) and P1 (48%) at the south, and C2 and P2 and (42-48%) at the center of both GC coastlines. Detailed information on macroalgae specimens collected (ecosystem, habitat, number of composite samples, morphological group, and taxon) is given as Supplementary Information (Table SI-1).

3.2. δ^{13}C-macroalgal variability in function of taxonomy and morpho-functional groups

The variability of δ^{13}C values in macroalgae was analyzed by taxon in the phylum, genus, species, and morphofunctional groups. δ^{13}C values analyzed by phylum showed a unimodal distribution with a peak at -14±1.4‰ (Fig 2 and 3), where Ochrophyta displayed the values from -21.5 to -2.2‰ (-12.5±3.7‰), significantly higher to Chlorophyta (-25.9 to -5.5‰, -14.5±3.0‰) and Rhodophyta that showed the largest range (-34.6 to -4.5‰, -14.8±3.9‰). The δ^{13}C-macroalgal values (average±SD) for the genus of Chlorophyta, Ochrophyta, and Rhodophyta (Fig. 3.) varied from -33.8±1.1‰ for *Schizymenia* to -7.8±0.7‰ for *Amphiroa*. Based on the highest values, specimens of three Phyla with relatively high δ^{13}C values (>-10‰), evidenced the presence of CCM's by active uptake of HCO_3^- (Fig. 3.). For example, in Chlorophyta, specimens belonging to genera like *Caulerpa, Cladophora,*

315 *Codium, Ulva*, while in Ochrophyta, $\delta^{13}C$ values >-10‰ were recorded in genera as *Colpomenia,*
316 *Dictyota, Padina, Sargassum*. In the case of Rhodophyta, high $\delta^{13}C$ values were observed in
317 calcifying macroalgae species like *Amphiroa* and *Jania* (showed in purple bars, Fig. 3c) but also in
318 fleshy macroalgae like *Gigartina*, *Hypnea*, and *Polysiphonia*. On the contrary, values lower than -
319 30‰ that denote uptake of CO_2 by diffusion, were observed only in Rhodophyta in *Schizymenia*
320 *Halymenia, and Gigartina*. Even so, most specimens showed $\delta^{13}C$ signals that evidence a mechanism
321 that uses a mix of HCO_3^- and CO_2 for photosynthesis.

322 A multiple comparison analyses revealed significant differences in the $\delta^{13}C$-macroalgal values
323 among genera, ordered as *Schizymenia* < *Polysiphonia* < *Ulva*, *Gracilaria* and *Spyridia* (-16.1±0.6‰
324 to -15.1±0.2‰) < *Gymnogongrus, Laurencia, Hypnea, Cladophora, Dictyota, Sargasumm,*
325 *Chaetomorpha*, and *Grateloupia* (from -15.4±0.7‰ to -13.8±0.8‰) < *Codium* and *Padina* (-
326 12.5±2.4‰ to -12.4±2.5‰) < *Colpomenia* and *Amphiroa* (-9.2±0.3 to -7.8±0.7‰) ($F=16.81$,
327 $p<0.001$).

328 Aggrupation of $\delta^{13}C$ values based on morpho-functional features on macroalgae id displayed in Fig.
329 4. The most representative groups in the phylum Chlorophyta varied from -15.8±0.3‰ for C-Tubular
330 to -12.4±0.5‰ for C-thallus erect. The phylum Ochrophyta includes O-Thick leathery with the
331 lowest mean (-14.8±0.3‰) and O-Hollow with a spherical or subspherical shape with the highest
332 values (-9.2±0.3‰). The lowest and highest $\delta^{13}C$ values for Rhodophyta were observed for R-
333 flattened macrophytes (-24.0 ± 9.6‰) and R-Larger-sized articulated coralline (-7.89±0.75‰),
334 respectively. Significant differences were observed among groups, which were ordered as follows:
335 R-flattened macrophytes<R-blade like < C-Tubular < O-Tick leathery and R-Large size corticated <
336 C-Blade like and C-Filamentous uniseriate < C-Erect thallus and O-Compressed with branch < O-
337 Hollow with spherical < R-Larger-sized articulated coralline.

High intraspecific variability in $\delta^{13}C$ signal for the more representative genera of each taxon is showed in Table 1-3. For *Codium*, *C. brandegeei* (11.8±1.2‰) and *C. simulans* (-11.4±2.2‰) showed higher $\delta^{13}C$ values than *C. amplivesculatum* (-14.4±2.7‰). *Colpomenia* species had higher $\delta^{13}C$ values than the other genera, with higher values for *C. tuberculata* (-8.7±3.2‰) than *Colpomenia* sp. (-10.9±3.6‰) and *C. sinuosa* (-10.2±2.9‰). *Gracilaria* showed comparable $\delta^{13}C$ values in the four species (from -16.4±1.6‰ for *G. pacifica* to -15.5±2.4‰ for *Gracilaria* sp.). *Hypnea* showed non-significant $\delta^{13}C$ differences in three representative species (-16.4±1.7‰ for *H. spinella* to -14.9±2.3‰ for *Hypnea* sp.). *Laurencia* sp. (-12.9±1.2‰) was higher than *L. pacifica* (-14.9±2.2‰), while *Padina* sp. (-11.1±1.5‰) higher than *P. durvillaei* (-13.2±2.6‰). *Sargassum* was one of the most diverse genera studied with six representative species, with $\delta^{13}C$ values ordered as follow: *S. horridum* = *S. sinicola* = *S. johnstoniis* (-15.5±2.9 to -15.1±2.4‰) < *S. lapazeanum* (-14.5±1.6‰) = *Sargassum* sp. (-14.2±2.3‰) < *S. herphorizum* (-13.6±1.6‰). *Spyridia* sp. (-17.0±1.2‰) and *S. filamentosa* (-15.8±3.8‰) showed non-significant differences. The six representative species of *Ulva* were divided into two morphological groups, filamentous and laminates. Filamentous species that averaged -16.3±2.0‰ for *U. clathrata*, -16.0±3.6‰ for *U. flexuosa*, -15.7±1.7‰ for *U. acanthophora* and -15.3±2.5‰ for *U. intestinalis* and *Ulva laminates* that included *U. linza* (-15.5±2.4‰) and *U. lactuca* (-14.1±3.1‰). Non-significant differences were observed between morphological groups and among species. A high intra-specific variability, 11-28%, explains average overlapping.

3.3. $\delta^{13}C$-macroalgal variability in coastal sectors

Despite that, each taxon recorded a different number of genus and species along the GC coast (SI1), the macroalgal assemblages according to their fico-floristic region also express differences in their carbon uptake strategies, and their proportion inferred by their $\delta^{13}C$ signal are shown in Fig. 5. Even

though most species inhabiting the GC coastal sectors displayed domination of strategies based on active CCM's, but the tendencies were different between taxa and coastal regions. The strategy that combined different sources of DIC were dominant in all regions and taxa (60-90%). Exceptions were observed in the P1 (68%) and C1 (37%) regions for Ochrophyta, where the specialized strategy of only HCO_3^- user were significant. The strategy based on only use of CO_2 was observed in the peninsular coast in P2 and P3 for Rhodophyta with 2-3.3%. Overall, more negative $\delta^{13}C$ values in macroalgae specimens' values of the same genus were observed at continental (C2) compared to peninsular coastline (P1-P3) and more negative southward than northward.

3.4. $\delta^{13}C$-macroalgal variability in function of taxonomy and habitat features and environmental conditions

Variability of $\delta^{13}C$ values for the most representative genera was evaluated by multiple comparative analyses in the habitat features' function, including the substrate, hydrodynamic, and emersion level. Large $\delta^{13}C$ variability observed between specimens of the same genus collected in the different habits does not show any significant pattern, and non-significant differences were observed. An exception was observed with the emersion level (showed in Fig. 6), where intertidal specimens recorded lesser negative values than subtidal in most macroalgae genus. For example, for *Hydroclathrus* (intertidal -5.7±0.9‰; subtidal -11.4±5.9‰), *Amphiroa* (intertidal -6.9±1.5; subtidal -9.9±6.1), *Hypnea* (intertidal -13.5±2.5‰; subtidal -18.6±1.8‰), and *Laurencia* (intertidal -13.5±1.3‰; subtidal -17.1±1.8‰). Exceptions were observed for *Polysiphonia* (intertidal -19.7±2.2‰, subtidal -14.9±6.7‰), *Spyridia* (intertidal -16.9±3.3‰, subtidal -13.2±0.7‰) and *Colpomenia* (intertidal -9.4±3.4‰, subtidal -7.7±1.3‰).

Non-significant differences were observed for the same genera at different temperatures ranges,

except for *Grateloupia* (cold, -19.2±4.7‰, typical -14.4±2.2‰, warm -14.5±2.2‰) and *Polysiphonia* (cold, -21.0±0.4‰, typical -18.1±5.5‰, warm -17.9±2.3‰) with more negative values in colder than warmer waters (F=6.42, p<0.001). Neither significant difference was observed in $\delta^{13}C$ values in macroalgae specimens from the different genus in the same temperature range. For example, *Colpomenia* (cold -8.3±2.4‰, typical -9.4±3.7‰, warm -9.2±2.6‰), *Codium* (cold -11.9±1.9‰, typical -12.5±3.0‰, warm -13.6±0.6‰), and *Padina* (cold -11.3±2.5‰, typical -11.8±1.7‰, warm -13.4±2.7‰) (Fig. 7a).

Significant differences were observed among genus related to the pH level at seawater (Fig. 7b). Under typical pH seawater, *Amphiroa* and *Colpomenia* were 1-2‰ more negatives than in alkaline waters, while *Ulva* and *Spyridia* were 3-5‰ less negative than in acidic waters. *Amphiroa* and *Colpomenia* were not collected in acidic water, and neither *Spyridia* in alkaline waters to compare. Another genus also showed extremes values between alkaline (*Tacanoosca* -7.6±1.0‰) and acidic waters (*Schizymenia*, -32.9±2.0‰). The following order was observed in the genus collect at the three pH ranges: alkaline > typical > acidic. Significant differences were observed for genus *Ahnfeltiopsis, Caulerpa, Gymnogongrus, Padina*, and *Ulva*, with higher values at alkaline than in acidic waters. Values of $\delta^{13}C$ for specimens of the same genus collected at typical pH waters are mostly overlapped between those for alkaline and acidic seawaters. Non-significant differences in $\delta^{13}C$ values were observed for *Grateloupia, Hypnea,* and *Polysiphonia* concerning pH-type waters.

We analyzed the carbon uptake strategies on macroalgal assemblages in the function of environmental factors like temperature, pH, and salinity (Fig. 8). Regarding the $\delta^{13}C$ variability for all data set in response to temperature and salinity, non-significant trend was observed between $\delta^{13}C$-macroalgal in both parameters' function. A poor but significant correlation was observed between $\delta^{13}C$ and pH ($R^2 = 0.04$) (Table 4). The proportion of specimens with a strategy of only HCO_3^- use

was different between environmental factors and taxa (previously described), for example, Ochrophyta showed the highest proportion (35%) in colder temperature, in pH-Alkaline (31%), and at typical salinity regimen (27%), while Chlorophyta enhanced to 30% in acid pH and Rhodophyta recorded 21% at normal seawater. The opposite strategy (only use of dissolved CO_2) that was observed only in Rhodophyta, the highest percentage was observed in estuarine salinity regimen (10%).

3.5. Variation latitudinal of δ^{13}C-macroalgal

The δ^{13}C-macroalgal variation in the GC biogeography was evaluated by regression linear analysis between δ^{13}C values along the nine degrees latitude in both GC coastlines. A non-significant latitudinal trend was observed for datasets, but for the three taxa's most representative genera, δ^{13}C values correlated with latitude (Fig. 9). In Chlorophyta, with the higher genera number, δ^{13}C values increased with latitude, with low but significant correlation. Contrarily, in Ochrophyta and Rhodophyta specimens, the δ^{13}C values decreased non-significantly with latitude.

Significant correlations ($p<0.001$) were observed for δ^{13}C-macroalgal *versus* latitude in the most representative morphofunctional groups (Fig. 10). Representative morphofunctional groups of Chlorophyta (e.g., C-Tubular, C-Filamentous uniseriate), showed a positive correlation, while those belonging to Ochrophyta (e.g., O-thick leathery;) and Rhodophyta (e.g., R-large sized corticated) showed a negative trend with latitude.

3.6. Analyses of δ^{13}C macroalgal variability

An analysis of the effects, independent and combined, on the δ^{13}C-macroalgal variability related to life form and environmental factors, was conducted. Firstly, simple linear regression analyses were performed to evaluate the dependent variable's prediction power (δ^{13}C-macroalgal) in the function

of several independent variables controlling the main macroalgae photosynthesis drivers (light, DIC, and inorganic nutrients). Regression coefficients were estimated for each fitted regression model, which is used as indicators of the quality of the regression (Draper and Smith, 1998; Burnham and Anderson, 2002) as was described in Methods; however, our results description focused on the coefficients of determination (R^2 and adjusted R^2). The coefficient R^2 describes the overall relationship between the independent variables X_i with the dependent variable Y (δ^{13}C-macroalgal), and it is interpreted as the % of contribution to the δ^{13}C variability. While the adjusted R^2 statistics compensate for possible confounding effects between variables.

Results of the analysis of the relationships between δ^{13}C with each independent variable are summarized in Table 4. Regarding the inherent macroalgae properties, Phyla explain only 8% variability, the morphofunctional properties 35%, and taxon by genus 46%, and by species 57%.

The biogeographical collection zone, in terms of coastline (continental vs. peninsular) and coastal sectors (C1-C3 and P1-P3), explained a maximum of 5% variability. Related to the habitat features, only the emersion level (6%) contributed to the δ^{13}C variability. The contribution of the seawater's environmental conditions was marginal for pH (4%) and negligible for temperature and salinity. A marginal reduction in the percentage of contribution was observed for Phyla (1%) and morphofunctional properties (1%), but significant for genus (5%) and species (10%).

Multiple regression analyses were also performed to interpret the complex relationships among δ^{13}C-macroalgal, considering the life form (morphofunctional and taxon by genus) and their responses to environmental parameters. Results for the fitted regression models performed for morphofunctional groups (Table 5) and genus (Table 6) evidenced that the effect of the coastal sector and pH ranges on the δ^{13}C-macroalgal increased the contribution by 9-10% each one. The emersion level increased by 5-6%, the contribution respect to individual effect of morphofunctional group and genus, the

452 temperature and pH in 1 and 3%, respectively, while salinity decreased by 1-2%. Adding the effect
453 of the biogeographical collection zone, represented by the coastline sector, to those for
454 morphofunctional group (Table 5) and genus (Table 7), a notable increase of 11-12% was observed.
455 The full model considering the combined effect of the coastline sector + Habitats features for
456 Morphofunctional group or Genus (Table 7), showed R^2 of 0.60 and 0.71. In contrast, Coastline
457 sector + Environmental conditions + Morphofunctional group or Genus the R^2 increased to 0.62 and
458 0.72, respectively. The interactive explanations of environmental factors increased the explanation
459 percentage of $\delta^{13}C$ variability; however, these contributions were significantly lower than the
460 explained by life forms, such as the morphofunctional properties and taxa by genus and species.
461 The combined effect of environmental condition on the $\delta^{13}C$ variability was tested for the best-
462 represented morphological groups and genus. Results evidenced that 9 of 21 morphological groups
463 showed significant effects on the $\delta^{13}C$ variability (Table 8), five increasing and four decreasing the
464 model constant of $\delta^{13}C$=-14.2‰. For example, for the O-Hollow with spherical or subspherical shape
465 (+4.9‰) and R-Larger-sized articulated corallines (+6.3‰), the predicted values are -7.9±0.8‰ and
466 -9.2±0.4‰. For R-Filamentous uniseriate and pluriseriate with erect thallus (-2.1‰) and C-Tubular
467 (-1.6‰), the predicted values are -16.3±0.5‰ and -15.8±0.5‰, respectively. Regarding taxon, a
468 significant effect was observed only in 13 genera, including *Colpomenia* (+5.4‰), *Amphiroa*
469 (+6.8‰), and *Padina* (+2.2‰) increasing the signal, and *Polysiphonia* (-3.7‰), *Gracilaria* (-0.9‰),
470 and *Spyridia* (-1.4‰) decreasing the signal of the model constant (Table 9). In 33 species was
471 observed a significant effect on the $\delta^{13}C$ variability, including *C. tuberculate* +5.9‰, *C. sinuosa*
472 +4.4‰, *H. pannosa* +4.4‰, *H. johnstonii* +4.4‰, and *Amphiroa spp*. (+4.4 to 8.2‰) increasing the
473 model constant $\delta^{13}C$= -14.6‰, and *Spyridia* sp. (-2.5‰), *G. filicina* (-2.3‰), *P. mollis* (-5.2‰) and
474 *S. pacifica* (-19.2‰) (Table 10).
475

3.7. Preliminary estimations of Δ^{13}C-macroalgal

Concurrent analysis of surface seawater for alkalinity, proportions of the chemical species of DIC (CO_2, HCO_3^-, and CO_3^{2-}), and δ^{13}C-DIC evidenced that δ^{13}C-DIC in GC seawater averages 1.4±0.4‰ (-1 to 4.9‰) (Fig. S1). In our preliminary data, the δ^{13}C-DICseawater slightly (in 0.5‰) decreased during the rainy season in those zones influenced by river discharges along the continental coastline, with non-significant differences among coastal sectors. δ^{13}C-DIC values in GC seawater are comparable to the averages 1.4-1.6‰ reported for the surface seawaters in the Eastern North Pacific in the 1970s-2000s period (Quay et al., 2003; Hinger et al., 2010; Santos et al., 2011).

Based on the subtraction of δ^{13}Cmacroalgae to δ^{13}C-DICseawater, the integrative discrimination factor against ^{13}C averaged 16.0±3.1‰, 16.8±4.3‰, and 14.0±3.8‰ for Phyla Chlorophyta, Rhodophyta, and Ochrophyta, respectively. Five groups were identified in function of the Δ^{13}C values, one for Chlorophyta (Δ^{13}C=16.0±3.1‰), two for Rhodophyta (16.6±3.8‰ and 34.6±1‰), and two for Ochrophyta (9.1±1.7‰ and 15.7±2.7‰) (Fig. S2). Values of Δ^{13}C were comparable to δ^{13}C of the thallus of macroalgae, thus δ^{13}C-macroalgal reflect mainly the discrimination during carbon assimilation. Like δ^{13}C-macroalgal, the Δ^{13}C values were subject to considerable variation.

4. Discussions

4.1. Explaining the δ^{13}C macroalgal variability

In this study, results revealed high variability in the δ^{13}C of the large inventory of macroalgae collected along GC coastline between five years period. A linear regression analysis of the effects of life form revealed that the δ^{13}C-macroalgal variability is mainly explained by taxonomic (genus

46%, species 57%) and morphofunctional groups. This result is consistent with the report of Lovelock et al., (2020), who found that 66% of $\delta^{13}C$ variability was explained by taxonomy. Even so, the variability associated with each genus is not the same and can be classified in three groups: 1) high variability (e.g., *Schizymenia* =±19.1‰), moderate variability (e.g., *Hydroclathrus*=±7.3‰; *Amphiroa* =±6.8‰) and low variability (e.g., *Gracilaria* =±0.89; *Spyridia* =±1.46‰).

Most authors studying the isotopic composition of C in macroalgae have reported the high isotopic variability, which has been attributable to the taxon-specific photosynthetic DIC acquisition properties (Raven et al., 2002a, Mercado et al., 2009, Marconi et al., 2011, Stepien, 2015, Díaz-Pulido et al., 2016; Lovelock et al., 2020). In our study, we observed that the intrinsic characteristics of each morpho-functional group of macroalgae (e.g., thallus structure, growth form, branching pattern, and taxonomic affinities) are determinant of the $\delta^{13}C$-macroalgal signals. Although non-evaluated in this study, the maturity of the specimens (e.g., young, adult, vs senescence) is also relevant (e.g., Carvalho et al., 2007; 2009b).

The $\delta^{13}C$-macroalgal depends on the carbon source ($\delta^{13}C$-DIC in seawater), the isotope discrimination during carbon assimilation in the photosynthesis ($\Delta^{13}C_p$<29‰ in a variable degree), and the plant respiration ($\Delta^{13}C_r$ average ±2.3‰) (Carvalho et al., 2009a,b, 2010; Carvalho and Eyre, 2011, Rautemberger et al., 2015). Comparatively, the $\Delta^{13}C_r$ value is relatively small regarding $\Delta^{13}C_p$, thus $\delta^{13}C$-macroalgal basically is an integrative value of the isotope discrimination during DICseawater assimilation [$\Delta^{13}C$= ($\delta^{13}C$-DIC seawater – $\delta^{13}C$macroalgae)] (Carvalho et al., 2009a). Based on the $\Delta^{13}C$ values, five groups were identified in our study: one for Chlorophyta ($\Delta^{13}C$=16.0±3.1‰), two for Rhodophyta (16.6±3.8‰ and 34.6±1‰), and two for Ochrophyta (9.1±1.7‰ and 15.7±2.7‰). Values of $\Delta^{13}C$ were comparable to $\delta^{13}C$ of the thallus of macroalgae, thus $\delta^{13}C$-macroalgal reflect mainly the discrimination during carbon assimilation. The $\delta^{13}C$-

macroalgal values reflect the discrimination during carbon assimilation attributable to the taxon-specific photosynthetic DIC acquisition properties. $\Delta^{13}C$-macrolgal variability, captured in the $\delta^{13}C$-macroalgal signals, is related to thickness of the boundary layer around the thallus (Raven et al. 1982), the leakage during carbon uptake (Sharkey and Berry 1985, Maberly et al. 1992), and photosynthetic intensity (Wiencke and Fischer 1990, Kübler and Raven 1994, 1995), and respiration rates (Carvalho et al., 2010; Carvalho and Eyre, 2011, Rautemberger et al., 2015). All intrinsic properties related to the life form.

Many species that recorded high $\delta^{13}C$ values (and low $\Delta^{13}C$ values) were fleshy macroalgae that are characterized to be bloom-forming macroalgae belonging to genera *Ulva, Gracilaria, Cladophora, Spyridia*, and *Sargassum* (Páez-Osuna et al., 2013, Valiela et al., 2018). It is not surprising, due to species with high photosynthetic activity and high relative growth rates (Hiraoka et al., 2020) have high carbon demand that results in lower isotopic discrimination against ^{13}C (Cornelisen, et al., 2007; Carvalho et al., 2010ab; Kübler and Dungeon, 2015; Rautemberger et al., 2015). Bloom-forming macroalgae (e.g., *Ulva, Gracilaria, Sargassum*) have been remarks as facultative species with the capacity to switch from C3 to C4 pathway (Valiela et al., 2018). C4 pathway reduces photorespiration, the antagonist process of RuBisCo, enhancing the DIC assimilation in 25-40% and increasing the $\delta^{13}C$ values (Ehleringer et al., 1991; Bauwe et al., 2010; Zabaleta et al., 2012). C4 pathway has more energy investment in CCM's than in RuBisCo protein content than C3 pathway (Young et al., 2016). Also, the reports of features of C4 or C4-like pathway in algae have increased in the last years (Roberts et al., 2007; Doubnerová and Ryslavá, 2011; Xu et al.., 2012, 2013). For example, high activity of keys enzymes of C4 metabolisms, such as pyruvate orthophosphate dikinase (PPDK), phosphoenolpyruvate carboxylase (PEPC), and phosphoenolpyruvate carboxykinase (PCK), has been described in many algae species. But the establishment of a true C4

543 pathway in marine algae is not clear since the massive changes in gene expression patterns seem to
544 be incomplete, and it is suggested that many marine algae have high plasticity to use a combination
545 of CCM to overcome Ci limitations (Roberts et al., 2007; Doubnerová and Ryslavá, 2011; Xu et al..,
546 2012, 2013). A Stepwise model of the path from C3 to C4 photosynthesis is explained by Gowik and
547 Westhoff (2011). More research is required on this topic considering the increasing the frequency,
548 intensity, and extension of bloom-forming macroalgae events worldwide (Teichberg et al., 2010;
549 Valiela et al., 2018) and in México (Ochoa-Izaguirre et al. 2007; Ochoa-Izaguirre and Soto-Jiménez
550 2015; Páez-Osuna et al., 2017).

551 Changes in the habitat features and environmental conditions, such as light intensity and DIC
552 availability, influencing the growth rate and photosynthetic intensity, have a strong influence on $\delta^{13}C$
553 signal (Carvalho et al., 2007, 2009; Carvalho and Eyre, 2011; Stepien, 2015; Mackey et al., 2015;
554 Rautenberger et al., 2015). The light intensity is the external factor with more influence on the $\Delta^{13}C$-
555 macroalgal due to the regulation of carbon assimilation intensity (Wefer and Killingley 1986, Cooper
556 and DeNiro 1989, Grice et al. 1996; Carvalho et al., 2009a,b). Experimental studies found the light
557 levels as a key factor affecting the $\delta^{13}C$ values, for example under saturating light conditions *Ulva*
558 switched from a carbon uptake of HCO_3^- and CO_2 to increased HCO_3^- use (Rautemberger et al.,
559 2015). Furthermore, field studies have shown that species growing in low light habitats as deep
560 subtidal tend to have more negative $\delta^{13}C$ values than those in higher light environments (Mercado et
561 al., 2009; Hepburn et al., 2011; Marconi et al., 2011; Stepien 2015; Cornwall et al., 2015, Díaz-
562 Pulido et al., 2016). In this study, intertidal specimens recorded lesser negative values than subtidal
563 in most macroalgae genus. However, the vertical effect in the $\delta^{13}C$ signal related to the light
564 limitation was not recorded in our study because only shallow habitats (non-light limited), were
565 considered.

δ^{13}C-DICseawater is reasonably uniform in surface seawater (-4.8 to 3.6‰, median 1.5‰), with δ^{13}C values for CO_2, HCO_3^-, and CO_3^{2-} nearly -10, -0.5 and 2‰, respectively (Mook et al., 1974; Kroopnick 1985). Exceptions can be expected where variations in the salinity, alkalinity, and proportions of the chemical species of DIC (CO_2, HCO_3^- or CO_3^{2-}) occur (e.g., in coastal environments influenced by river and groundwater discharges) (Mook et al., 1974; Chanton and Lewis 1999; Hinger et al., 2010; Carvalho et al., 2015). Regarding DIC sources for macroalgae in the GC surface seawater, the availability, chemical proportions and δ^{13}C-DIC, were also relatively constant and uniform. Thus, the influence of the δ^{13}C-DIC variations to the δ^{13}C-macroalgal variability is negligible in the GC.

The effect of other environmental factors, such as salinity and pH, on δ^{13}C-macroalgal signals were evaluated. Regarding salinity, the influence of freshwater discharge by rivers and groundwater decreases the δ^{13}C signal, which could be explained by the effect of the reduction in the salinity regimen that follows a decrease in δ^{13}C-DIC in water (Hinger et al., 2010; Santos et al., 2011). In our study, non-significant correlation between δ^{13}C-macroalgal and salinity was observed.

Based on pH, differences in δ^{13}C were found only for a few genera (e.g., *Amphiroa, Colpomenia, Ulva, Spyridia*), with a trend to increase in the δ^{13}C values with pH increase, such as was reported by Maberly et al. (1992) and Raven et al. (2002b). Similar results were reported for Cornwall et al. (2017) in the field study, with the differential response of the δ^{13}C signals to pH among 19 species, in which only four species were sensitive to pH changes. Based on the complete dataset, a very weak but significant positive linear regression was observed between δ^{13}C and pH. Also, a trend to decrease in the δ^{13}C was recorded in the follow order: alkaline > typical > acidic. According to Stepien (2015), the result of meta-analyzes between pH values and δ^{13}C was positive only for Rhodophyta and Ochrophyte, but not for Chlorophyta. About 86% of the Stepien metadata met the

theoretical CCM assignation based on both parameters, exceptions for species with $\delta^{13}C$<-30‰ that have been capable of raising pH>9. A strong association between pH compensation point and $\delta^{13}C$ was reported by Iñiguez et al. (2009) in three taxa of polar macroalgae.

4.2. Using $\delta^{13}C$-macroalgal to infer carbon uptake strategies

In our study, the $\delta^{13}C$ signal from the thallus of macroalgae was used to infer carbon strategies. This tool was first used in macroalgal shallows communities of the Gulf of California. Most macroalgae species displayed $\delta^{13}C$ values that exhibit an active CCM's. About of 84% of the total analyzed specimens showed the facultative uptake of HCO_3^- and CO_2, the most common strategy identified in macroalgal shallow communities (Hepburn et al., 2011; Cornwall et al., 2015; Stepien 2015; Díaz-Pulido et al., 2016). Based on the carbon uptake strategies, the most abundant macroalgae were those able to use both HCO_3^- and/or CO_2 by means of active uptake plus passive diffusion (strategy 2: -10<$\delta^{13}C$>-30‰).

Macroalgae collected in GC also involved those that are only HCO_3^- users (strategy 1: $\delta^{13}C$>-10‰) and those relying on diffusive CO_2 uptake (strategy 3: $\delta^{13}C$<-30‰). Photosynthesis that relies on CO_2 uptake (lack of CMM), the most primitive mechanism (Cerling et al., 1993), has fewer energy costs than HCO_3^- uptake that requires complex machinery with a high operational cost (Giordano et al., 2005; Hopkinson et al., 2011; Hopkinson, 2014; Raven and Beardall, 2016). The energy for macroalgae to uptake HCO_3^-, cross the plasma membrane, and covert to CO_2 for photosynthesis, is obtained through irradiance (Cornelisen et al., 2007). Based on our sampling effort, focused on intertidal and shallow subtidal habitats featured by high-light intensities, we expected high proportions of species and specimens with the carbon uptake strategy that use only HCO_3^-. Results evidenced that strategy 1 was recorded in specimens belonging to 58 species of 170 total species.

The higher proportions of CCM species (HCO_3^- users), with high-energetic requirements, is explained by those elevated irradiances (Hepburn et al. 2011; Cornwall et al. 2015). Ochrophyta showed the highest proportion of species and specimens that depend only on HCO_3^- uptake on both coastlines in the southern region of GC (P1, C1). These differences can be partially explained by the low solubility of CO_2 due to relatively high temperatures in subtropical waters (Zeebe and Wolf-Gladrow, 2007) that impulse the development of CCM (Raven et al., 2002b) and by the high affinity to DIC by Ochrophyta, such as has been described before by Diaz-Pulido et al, (2016).

Only three non-calcifying species (*Schizymenia pacifica*, *Halymenia* sp., *Gigartina* sp.) belonging to Rhodophyta were CO_2 exclusive users ($\delta^{13}C$=-33.2±1‰). Based on measurements of pH drift, Murru and Sandgreen (2004), reported to *Schizymenia pacifica* and two species of Halymenia (e.g., *H. schizymenioides and H. gardner*) as restricted CO_2 users. Measurements of $\delta^{13}C$ in *Halymenia dilatate* confirmed the CO_2-restricted photosynthesis in specimens collected offshore in deep reefs of the Great Barrier reef (Díaz-Pulido et al., 2016). Red macroalgae that lack CCM, tend to inhabit low-light habitats like subtidal or low intertidal and are abundant in cold waters (Kübler et al., 1999, Raven et al., 2002a, Cornwall et al., 2015). According to these authors, approximately 35% of the total red algae tested on a global scale are strictly CO_2 dependents. The percentage of macroalgae species representative of Arctic and Antarctic ecosystems that lack CCM is 42-60% (Raven et al., 2002b; Iñiguez et al., 2019), 50% for temperate waters of New Zealand (Hepburn et al., 2011), and up to 90% found for a single site of Tazmania Australia (Cornwall et al., 2015). In our study, 91 red macroalgae species were sampled (of 453 red macroalgae species reported in the GC, Pedroche and Sentíes, 2003), of which <3% were CO_2 dependents. This low percentage could be related to the fact that deep habitats (>2 m depth low tide) were not explored in our surveys.

In our study, few calcifying macroalgae species using HCO_3^- and diffusive CO_2 (strategy 4) were

also collected, including the genera *Amphiroa* (-7.8±3.7‰) and *Jania* (-9.4±0.7‰), both Rhodophyta with articulated-form. *Padina*, a genus with less capacity to precipitate $CaCO_3$ (Ilus et al., 2017), displayed relatively high $\delta^{13}C$ values (-12.5±2.4‰) suggesting the presence of CCM using HCO_3^- exclusively. Three genera are very common in the GC. Stepien (2015) reported a global mean of -14.8±1.0‰ for calcifying species compared to -20.1±0.3‰ for non-calcifying species. Calcifying species have a different carbon uptake strategy influenced by the calcifying process that results in elevated $\delta^{13}C$ signals (Diaz-Pulido et al., 2016). High $\delta^{13}C$ values for calcifying species are related to the excess of H^+ released as residuals products of the calcifying process, also the acidified boundary layers benefit the HCO_3^- uptake (McConnaughey and Whelan 1997, Courneau et al., 2012). The high $\delta^{13}C$ values can also be related to the highly efficient light properties that are enhanced by the carbonate skeleton, resulting in an optimization of photosynthetic activity (Vasquez-Elizondo et al., 2017). Hofmann and Heesch (2018) reported high $\delta^{13}C$ values in eight rhodoliths species (calcifying species) for the organic matter thallus and thallus including $CaCO_3$ structure collected in deep habitats (25-40 m) where light availability is very low. Because the ocean acidification in progress, negative impacts are expected on calcifying organisms, more attention as ecological sentinels is warranted in the GC.

Based on the $\delta^{13}C$ values, it is possible to assume that at least one basal CCM is active, however, it is impossible to discern what type of CCM is expressed in the organisms (e.g., direct HCO_3^- uptake by the anion-exchange protein AE; Drechsler and Beer 1991; Drechsler et al. 1993) or types of mitochondrial carbonic anhydrase (e.g., internal and external) that enhance the fixation of Ci by recycling mitochondrial CO_2 (Bowes, 1969; Zabaleta et al., 2012; Jensen et al., 2020). Also, the co-existence of different CCMs has been described for the same species (Axelsson et al., 1999, Xu et al., 2012), even that different CCM's can operate simultaneously, generating different Ci

contribution to RuBisCo internal pool (Rautemberger et al., 2015). The variety of CCMs and their combinations could contribute to the high $\delta^{13}C$ variability for the same species. In our field study, it is impossible to explain the variations of $\delta^{13}C$ or $\Delta^{13}C$-macroalgal relative to CCM or CA activity types. Controlled experiments, as those conducted by Carvalho and collaborators (e.g., Carvalho et al 2009a,b, 2010), are required to obtain this knowledge.

4.3. Variability of $\delta^{13}C$ macroalgal between the GC bioregions

Changes in the $\delta^{13}C$ signal with latitude, mainly related to the light and temperature, have been reported in the literature (Mercado et al., 2009; Marconi et al., 2011; Stepien, 2015; Hofmann and Heesch, 2018; Lovelock et al., 2020). For example, a negative correlation between latitude and $\delta^{13}C$-macroalgal was described by Stepien (2015), concluding that the $\delta^{13}C$ signal increased by 0.09‰ for each latitude degree from the Equator. Hofmann and Heesch (2018) recently showed a strong decrease in latitudinal effect (R^2= 0.43 $\delta^{13}C_{total}$ and 0.13, for $\delta^{13}C_{organic\text{-}tissue}$, p=0.001) for rhodolite of the northern hemisphere and macroalgae from coral reefs in Australia. In both cases, the latitude range is higher than we tested (30º to 80º and from 10º to 45º, respectively). These differences on a big scale tend to be associated with a temperature effect (Stepien, 2015) and their effect on CO_2 solubility in seawater (Zeebe and Wolf-Gladrow, 2007). However, in our study, any geographical pattern in the $\delta^{13}C$ macroalgal was observed. Our linear regression analyzes for latitudes showed a low but significant correlation for the dataset classified by morphofunctional groups and genus, negative in the cases of Rhodophyta and Ochrophyta groups, and positive for Chlorophyta.

Non-defined patterns may be explained by non-significant variations in light and temperature along the GC latitudes. In fact, most of the shallow habitats occupied by macroalgal communities in the GC were high-light environments with narrow ranges in temperature. However, the combined effect

of the coastline sector, habitats feature, or environmental condition for Morphofunctional group or Genus explained 60-62 and 71-72% of the $\delta^{13}C$ variability, respectively. Life forms, such as the morphofunctional properties and taxa by genus and species, constitute the main contributors to the variability. Our analysis of variability for the best-represented morphological groups (e.g., R-Filamentous uniseriate and pluriseriate with erect thallus and C-Tubular) and genus (e.g., *Colpomenia*, *Padina*, *Polysiphonia* and *Gracilaria*) revealed that certain life forms are better monitors explaining the variability of $\delta^{13}C$-macroalgal (and $\Delta^{13}C$ values) than others. However, more research is required to better interpretation to evaluate the isotope discrimination during carbon assimilation and respiration across the macroalgae lifecycle.

The proportion of specimens with different carbon uptake strategies also showed regional variations. For example, the facultative uptake of HCO_3^- and CO_2 was dominant in the macroalgal shallow communities in the GC (60 to 90% of specimens), with an exception in the P1 region for Ochrophyta where the specialized strategy of only HCO_3^- use dominated (68%), and high proportion were observed in C1 with 37%. While the strategy based on only use of CO_2 was observed in the peninsular coast in P2 and P3 for Rhodophyta with 2-3.3%. Finally, the coastal sector C2 showed more negative $\delta^{13}C$ values in macroalgae specimens of the same genus compared to peninsular coastline (P1-P3). Small but detectable changes were observed in the Phyla distribution based on environmental conditions. For example, Ochrophyta showed the highest proportion (35%) in colder temperature, in pH-Alkaline (31%), and at typical salinity regimen (27%), while Chlorophyta enhanced to 30% in acid pH and Rhodophyta recorded 21% at normal seawater. The opposite strategy (only use of dissolved CO_2) that was observed only in Rhodophyta, the highest percentage was observed in estuarine salinity regimen (10%). Again, more research is required to obtain useful information on the physiological and environmental status of macroalgae.

5. Conclusions

In conclusion, we observed high δ^{13}C-macroalgal variability in macroalgae communities in the Gulf of California, such as has been reported in other worldwide marine ecosystems. Life form is the principal cause of δ^{13}C-macroalgal variability, and taxonomy and morphology explain up to 57% and 35% of the variability, respectively. Changes in habitat characteristics and environmental conditions also influence the δ^{13}C-macroalgal variability. The full model considering the combined effect of the life form, coastline sector, and environmental conditions explains up to 62% (morphological groups) and 72% (genus) of the variability. The effect of the coastal sector, pH ranges, and emersion level were significant, while for salinity and temperature negligible.

Most macroalgae inhabiting in GC displayed the presence of CO_2 carbon mechanisms to uptake HCO_3^- for photosynthesis, 84% of the total analyzed specimens were able to use both HCO_3^- and/or CO_2 employing active uptake plus passive diffusion (strategy 2: $-10<\delta^{13}C>-30‰$). Specimens belonging to 58 species of 170 total species showed carbon uptake strategy 1 that use only HCO_3^-. A higher proportion of CCM species (HCO_3^- users) was expected because we focused on intertidal and shallow subtidal habitats featured by high-light intensities. Only three non-calcifying species (*Schizymenia pacifica*, *Halymenia* sp., *Gigartina* sp.) belonging to Rhodophyta (3%) were CO2 exclusive users (strategy 3: $\delta^{13}C<-30‰$). The low percentage of CO_2 dependents versus 40-90% reported for temperate regions could be related to the shallow habitat sampled in our surveys (<2 m depth low tide). The calcifying macroalgae genera *Amphiroa* and *Jania* using HCO_3^- and diffusive CO_2 influenced by the calcification process (strategy 4) were present in the macroalgal communities along the GC and high δ13C values (similar to strategy 1). Because the ongoing ocean acidification, these calcifying organisms constitute excellent ecological sentinels in the GC.

724 Finally, diverse authors have reported significant correlations between $\delta^{13}C$ signal and latitude,
725 mainly related to the light and temperature. However, in the latitude range (21º-31ºN) in our study,
726 the linear regression analyzes showed a low correlation for the $\delta^{13}C$-macroalgal dataset classified by
727 morphofunctional groups and genus, being negative for Rhodophyta and Ochrophyta and positive
728 for Chlorophyta. Because the shallow habitats occupied by macroalgal communities in the GC were
729 high-light environments with narrow ranges in temperature, not clear patterns along the GC latitudes.
730 However, detectable changes were observed in the d13C-macroalgal and the proportion of specimens
731 with different carbon uptake strategies among coastal sectors. For example, the facultative uptake of
732 $HCO3^-$ and CO_2 was dominant in the macroalgal shallow communities in the GC (60 to 90% of
733 specimens), but in the coastal sector P1 was the specialized strategy of only HCO_3^- use the dominant
734 strategy (68%), and significant at C1 (37%).

735 Our research is the first approximation to understand the $\delta^{13}C$-macroalgal variability in one of the
736 most diverse marine ecosystems in the world, the Gulf of California. We did not pretend to resolve
737 the intricate processes controlling the variations of $\delta^{13}C$ or $\Delta^{13}C$-macroalgal during carbon
738 assimilation and respiration and determine the isolated influence of each environmental factor.
739 Controlled experiments in laboratory and mesocosm type in combination with field studies are
740 required to elucidate the complex processes controlling the δ13C-macroalgal. Even so, the $\delta^{13}C$-
741 macroalgal was a good proxy to identify CO_2 or HCO_3^- source in photosynthesis and to infer the
742 presence or absence of CCM's and identify the macroalgae lineages that could be in competitive
743 advantage based on their carbon uptake strategy and identify their geographical distribution along
744 GC.

745 Under the current conditions of climate change and their effects as ocean acidification in progress
746 and the bloom-forming macroalgae events that increases in México and worldwide, the analysis of

747 δ13C-macroalgal constitute an excellent tool to help to predict the prevalence and shift of species in
748 a macroalgal communities' focused on carbon metabolism.

749 **6. Data Availability Statement**

750 Data set are each permanently deposited Soto-Jimenez, MARTIN F; Velázquez-Ochoa, Roberto;
751 Ochoa Izaguirre, Maria Julia. Earth and Space Science Open Archive ESSOAr; Washington, Nov
752 25, 2020. DOI:10.1002/essoar.10504972.1

753 https://search.proquest.com/openview/2060de58b217ca47495469b53ae2f347/1?pq-
754 origsite=gscholar&cbl=4882998

755 **7. Author contribution**

756 Velázquez-Ochoa R. participate in the collection, processing, and analysis of the samples as a part
757 of his master's degree thesis. Ochoa-Izaguirre J. also participate in sample collections and
758 identified macroalgae specimens. Soto-Jiménez M.F. coordinated the research, was the thesis
759 director, and prepared the manuscript with contributions from all co-authors.

760 **8. Competing interests**

761 The authors declare that they have no conflict of interest.

762 **9. Acknowledgements**

763 The authors would like to thank H. Bojórquez-Leyva, Y. Montaño-Ley, and A. Cruz-López for
764 their invaluable assistance with field and laboratory work. Thanks to S. Soto Morales for the
765 English revision. UNAM-PAPIIT IN206409 and IN208613 provided financial support and
766 UNAM-PASPA supported to MF Soto-Jimenez for Sabbatical year.

10. References

Abbot, I. A., and Hollenberg, G.: Marine algae of California. Standford University Press, California. 1976.

Aguilar-Rosas, L. E., and R. Aguilar-Rosas, R.: Ficogeografía de las algas pardas (Phaeophyta) de la península de Baja California, in: Biodiversidad Marina y Costera de México (Comisión Nacional Biodiversidad y CIQRO, México), edited by: Salazar-Vallejo, S. I. and González, N. E., 197-206, 1993.

Aguilar-Rosas, L. E., Pedroche, F. F., and Zertuche-González, J. A.: Algas Marinas no nativas en la costa del Pacífico Mexicano. Especies acuáticas invasoras en México. Comisión Nacional para el Conocimiento y Uso de la Biodiversidad, México, 211-222, 2014.

Álvarez-Borrego, S.: Gulf of California., in: Ecosystems of the World, 26. *Estuaries and Enclosed Seas,* (Elsevier, Amsterdam), Edited by: Ketchum BH., 427–449, 1983.

Anthony, K. R., Ridd, P. V., Orpin, A. R., Larcombe, P., and Lough, J.: Temporal variation of light availability in coastal benthic habitats: Effects of clouds, turbidity, and tides, Limnol. Oceanogr., 49(6), 2201-2211, https://doi.org/10.4319/lo.2004.49.6.2201, 2004.

Axelsson, L., Larsson, C., and Ryberg, H.: Affinity, capacity and oxygen sensitivity of two different mechanisms for bicarbonate utilization in *Ulva lactuca* L. (Chlorophyta), Plant Cell Environ., 22, 969–978, https://doi.org/10.1046/j.1365-3040.1999.00470.x, 1999.

Balata, D., Piazzi, L., and Rindi, F.: Testing a new classification of morphological functional groups of marine macroalgae for the detection of responses to stress, Mar. Biol., 158, 2459–2469, https://doi.org/10.1007/s00227-011-1747-y, 2011.

Bastidas-Salamanca, M., Gonzalez-Silvera, A., Millán-Núñez, R., Santamaria-del-Angel, E., and Frouin, R.: Bio-optical characteristics of the Northern Gulf of California during June 2008, Int. J. Oceanogra., https://doi.org/10.1155/2014/384618, 2014.

Bauwe, H., Hagemann, M., and Fernie, A. R.: Photorespiration: players, partners and origin, Trends Plant Sci., 15(6), 330–336, https://doi.org/10.1016/j.tplants.2010.03.006, 2010.

793 Beardall, J., and Giordano, M.: Ecological implications of microalgal and cyanobacterial CO_2
794 concentrating mechanisms, and their regulation, Funct. Plant Biol., 29(3), 335–347,
795 https://doi.org/10.1071/PP01195, 2002.

796 Bold, C. H., and Wynne, J. M.: Introduction to the Algae: Structure and reproduction. Prentice-Hall,
797 Incorporated, 1978.

798 Bowes, G. W.: Carbonic anhydrase in marine algae, Plant Physiol., 44:726–732,
799 https://doi.org/10.1104/pp.44.5.726, 1969.

800 Bray, N. A.: Thermohaline circulation in the Gulf of California, *J. Geophys. Res*. *Oceans.*, 93(C5),
801 4993–5020, https://doi.org/10.1029/JC093iC05p04993, 1988.

802 Brodeur, J. R., Chen, B., Su, J., Xu, Y. Y., Hussain, N., Scaboo, K. M., Zhang, Y., Testa, J. M. and
803 Cai, W. J.: Chesapeake Bay inorganic carbon: Spatial distribution and seasonal variability, Front.
804 Mar. Sci., https://doi.org/10.3389/fmars.2019.000996, 99, 2019.

805 Brusca, R. C., Findley, L. T., Hastings, P. A., Hendrickx, M. E., Cosio, J. T., and van der Heiden, A.
806 M.: Macrofaunal diversity in the Gulf of California. Biodiversity, ecosystems, and conservation in
807 Northern Mexico, 179, 2005.

808 Burnham, K. P., and Anderson, D. R.: A practical information-theoretic approach, Model selection
809 and multimodel inference, 2nd ed. Springer, New York, 2. 2002.

810 Carrillo, L., and Palacios-Hernández, E.: Seasonal evolution of the geostrophic circulation in the
811 northern Gulf of California, Estuar. Coast. Shelf Sci., 54(2), 157–173,
812 https://doi.org/10.1006/ecss.2001.0845, 2002.

813 Carvalho, M. C. and Eyre, B. D.: Carbon stable isotope discrimination during respiration in three
814 seaweed species, Mar. Ecol. Prog. Ser., 437:41–49. https://doi.org/10.3354/meps09300, 2011.

815 Carvalho, M. C., Hayashizaki, K., Ogawa, H., and Kado, R.: Preliminary evidence of growth
816 influence on carbon stable isotope composition of *Undaria pinnatifida,* Mar. Res. Indones., 32, 185-
817 188, 2007.

818 Carvalho, M. C., Hayashizaki, K., and Ogawa, H.: Effect of pH on the carbon stable isotope

819 fractionation in photosynthesis by the kelp *Undaria pinnatifida*, Coast. Mar. Sci, 34(1), 135-139,
820 2010a.

821 Carvalho, M. C., Hayashizaki, K. I., and Ogawa, H.: Temperature effect on carbon isotopic
822 discrimination by *Undaria pinnatifida* (Phaeophyta) in a closed experimental system[1], J. Phycol,
823 46(6), 1180-1186, https://doi.org/10.1111/j.1529-8817.2010.00895.x, 2010b.

824 Cerling, T. E., Wang, Y., and Quade, J.: Expansion of C4 ecosystems as an indicator of global
825 ecological change in the late Miocene, *Nature*, 361 (6410), 344–345,
826 https://doi.org/10.1038/361344a0, 1993.

827 Comeau, S., Carpenter, R. C., and Edmunds, P. J.: Coral reef calcifiers buffer their response to ocean
828 acidification using both bicarbonate and carbonate, *Proc. Bio. Sci.,* 280(1753), 20122374,
829 https://doi.org/10.1098/rspb.2012.2374, 2012.

830 CNA (Comisión Nacional del Agua): Atlas del agua en México, 2012.

831 Cornelisen, C. D., Wing, S. R., Clark, K. L., Hamish Bowman, M., Frew, R. D., and Hurd, C. L.:
832 Patterns in the $\delta^{13}C$ and $\delta^{15}N$ signature of *Ulva pertusa:* interaction between physical gradients and
833 nutrient source pools, Limnol. Oceanogr, 52(2), 820-832, 2007.

834 Cornwall, C. E., Revill, A. T., and Hurd, C. L.: High prevalence of diffusive uptake of CO_2 by
835 macroalgae in a temperate subtidal ecosystem, Photosynth. Res., 124, 181–190,
836 https://doi.org/10.1007/s11120-015-0114-0, 2015.

837 Dawson, E. Y.: The marine algae of the Gulf of California, Allan Hancock Pac. Exped., 3(10), [i-
838 v+] 189–453, 1944.

839 Dawson, E. Y.: Marine red algae of Pacific México. Part 2. *Cryptonemiales* (cont.), Allan Hancock
840 Pac. Exped., 17(2), 241–397, 1954.

841 Dawson, E. Y.: How to know the seaweeds, Dubuque, Iowa, USA. W.M.C. Brown. Co. Publishers.
842 pp 197., 1956.

843 Dawson, E. Y.: The marine red algae of Pacific Mexico, Part 4, Gigartinales. Allan Hancock Pacific
844 Exped., 2, 191-343, 1961.

Dawson, E. Y.: Marine red algae of Pacific México. Part 7. *Ceramiales*: Ceramiaceae, Delesseriaceae, Allan Hancock Pac. Exped., 26(1), 1–207, 1962.

Dawson, E. Y.: Marine red algae of Pacific México. Part 8. *Ceramiales*: Dasyaceae, Rhodomelaceae. Nova Hedwigia, 6, 437–476, 1963.

Díaz-Pulido, G., Cornwall, C., Gartrell, P., Hurd, C., and Tran, D. V.: Strategies of dissolved inorganic carbon use in macroalgae across a gradient of terrestrial influence: implications for the Great Barrier Reef in the context of ocean acidification, Coral Reefs, 35(4), 1327-1341, https://doi.org/10.1007/s00338-016-1481-5 2016.

Doubnerová, V., and Ryšlavá, H.: What can enzymes of C4 photosynthesis do for C3 plants under stress?, *Plant Sci.*, 180(4), 575–583, https://doi.org/10.1016/j.plantsci.2010.12.005, 2011.

Draper, N. R., and Smith, H.: Applied regression analysis, edited by: John Wiley & Sons (Vol. 326), 1998.

Drechsler, Z., and Beer, S.: Utilization of inorganic carbon by *Ulva lactuca*. *Plant Physiol.,* 97, 1439–1444, https://doi.org/10.1104/pp.97.4.1439, 1991.

Drechsler, Z., Sharkia, R., Cabantchik, Z. I., and Beer, S. Bicarbonate uptake in the marine macroalga *Ulva* sp. is inhibited by classical probes of anion exchange by red blood cells, *Planta*, 191(1), 34–40, https://doi.org/10.1007/BF00240893, 1993.

Dreckmann, K. M.: El género *Gracilaria* (Gracilariaceae, Rhodophyta) en el Pacífico centro-sur mexicano, Monografías ficológicas, 1, 77-118, 2002.

Dudgeon, S. R., Davison, I. R., and Vadas, R. L. Freezing tolerance in the intertidal red algae *Chondrus crispus* and *Mastocarpus stellatus:* Relative importance of acclimation and adaptation, Mar Biol., 106(3), 427–436, https://doi.org/10.1007/BF01344323, 1990.

Dudley, B. D., Barr, N. G., and Shima, J. S.: Influence of light intensity and nutrient source on $\delta^{13}C$ and $\delta^{15}N$ signatures in *Ulva pertusa,* Aquat. Biol., 9(1), 85–93, https://doi.org/10.3354/AB00241, 2010.

Ehleringer, J. R., Sage, R. F., Flanagan, L. B., and Pearcy, R. W.: Climate change and the evolution

of C4 photosynthesis, Trends Ecol. Evol., 6(3), 95–99, https://doi.org/10.1073/pnas.1718988115, 1991.

Enríquez, S., and Rodríguez-Román, A.: Effect of water flow on the photosynthesis of three marine macrophytes from a fringing-reef lagoon, *Mar. Ecol. Prog. Ser.*, 323, 119–132, https://doi.org/10.3354/meps323119, 2006.

Espinoza-Avalos, J.: Macroalgas marinas del Golfo de California, Biodiversidad marina y costera de México (CONABIO- CIQRO, México), edited by: Salazar-Vallejo, S.I., González, N. E., 328–357, 1993.

Espinosa-Carreón, T. L., and Valdez-Holguín, E.: Variabilidad interanual de clorofila en el Golfo de California. Ecol. Apl., 6(1-2), 83–92, 2007.

Espinosa-Carreón, T. L., and Escobedo-Urías, D.: South region of the Gulf of California large marine ecosystem upwelling, fluxes of CO_2 and nutrients, Environ Dev., 22, 42–51, https://doi.org/10.1016/j.envdev.2017.03.005, 2017.

Gateau, H., Solymosi, K., Marchand, J., and Schoefs, B.: Carotenoids of microalgae used in food industry and medicine. Mini-Rev. Med. Chem., 17(13), 1140–1172, https://doi.org/10.2174/1389557516666160808123841, 2017.

Gilbert, J. Y., and Allen, W. E.: The phytoplankton of the Gulf of California obtained by the ‘‘E.W. Scripps’’ in 1939 and 1940, J. Mar. Res., 5, 89–110, https://doi.org/10.1016/0022-0981(67)90008-1, 1943.

Giordano, M., Beardall, J., and Raven, J. A.: CO_2 concentrating mechanisms in algae: mechanisms, environmental modulation and evolution, Annu. Rev. Plant Biol., 66:99–131, https://doi.org/10.1146/annurev.arplant.56.032604.144052, 2005.

Gowik, U., and Westhoff, P.: The path from C3 to C4 photosynthesis, Plant Physiol., 155(1), 56–63, https://doi.org/10.1104/pp.110.165308, 2012.

Hepburn, C. D., Pritchard, D. W., Cornwall, C. E., McLeod, R. J., Beardall, J., Raven, J. A., and Hurd, C. L.: Diversity of carbon use strategies in a kelp forest community: implications for a high CO_2 ocean, Glob. Change Biol., 17, 2488–2497. https://doi.org/10.1111/j.1365-2486.2011.02411.x.,

2011.

Hinger, E. N., Santos, G. M., Druffel, E. R. M., and Griffin, S.: Carbon isotope measurements of surface seawater from a time-series site off Southern California, Radiocarbon 52(1):69–89, 2010.

Hofmann, L., and Heesch, S.: Latitudinal trends in stable isotope signatures and carbon-concentrating mechanisms of northeast Atlantic rhodoliths, Biogeosciences, 15, 6139–6149, https://doi.org/10.5194/bg-15-6139-2018, 2018.

Hopkinson, B. M., Dupont, C. L., Allen, A. E., and Morel, F. M. M.: Efficiency of the CO_2-concentrating mechanism of diatoms, Proc. Natl. Acad. Sci. U.S.A., 108, 3830–3837, https://doi.org/10.1073/pnas.1018062108, 2011.

Hopkinson, B. M., Young, J. N., Tansik, A. L., and Binder, B. J.: The minimal CO_2 concentrating mechanism of *Prochlorococcus* MED4 is effective and efficient, *Plant Physiol.*, 166, 2205–2217, https://doi.org/10.1104/pp.114.247049, 2014.

Hu, X., Burdige, D. J., and Zimmerman, R. C.: $\delta^{13}C$ is a signature of light availability and photosynthesis in seagrass, Limnol. Oceanogr., 57(2), 441–448, https://doi.org/10.4319/lo.2012.57.2.0441, 2012.

Hurd, C. L.: Water motion, marine macroalgal physiology and production, J. Phycol., 36, 453–472, https://doi.org/10.1046/j.1529-8817.2000.99139.x, 2000.

Iluz, D., Fermani, S., Ramot, M., Reggi, M., Caroselli, E., Prada, F., Dubinsky, Z., Goffredo, S. and Falin, G.: Calcifying response and recovery potential of the brown alga *Padina pavonica* under ocean acidification, ACS Earth Space Chem., 1(6), 316–323, https://doi.org/10.1021/acsearthspacechem.7b00051, 2017.

Iñiguez, C., Galmés, J., and Gordillo, F. J.: Rubisco carboxylation kinetics and inorganic carbon utilization in polar versus cold-temperate seaweeds, J. Exp. Bot., 70(4), 1283–1297. https://doi.org/10.1093/jxb/ery443, 2019.

Jensen, E. L., Maberly, S. C., and Gontero, B.: Insights on the functions and ecophysiological relevance of the diverse carbonic anhydrases in microalgae, Int. J. Mol. Sci., 21(8), 2922, https://doi.org/10.3390/ijms21082922, 2020.

925 Johansson, G., and Snoeijs, P.: Macroalgal photosynthetic responses to light in relation to thallus
926 morphology and depth zonation, Mar. Ecol. Prog. Ser., 244, 63-72, https://doi:10.3354/meps244063,
927 2002.

928 Kim, M. S., Lee, S. M., Kim, H. J., Lee, S. Y., Yoon, S. H., and Shin, K. H.: Carbon stable isotope
929 ratios of new leaves of *Zostera marina* in the mid-latitude region: implications of seasonal variation
930 in productivity, J. Exp. Mar Biol. Ecol*.,* 461, 286–296, https://doi.org/10.1016/j.jembe.2014.08.015,
931 2014.

932 Klenell, M., Snoeijs, P., and Pedersen, M.: Active carbon uptake in *Laminaria digitata* and *L.*
933 *saccharina* (Phaeophyta) is driven by a proton pump in the plasma membrane, *Hydrobiologia,* 514,
934 41–53, https://doi.org/10.1023/B:hydr.0000018205.80186.3e, 2004.

935 Kübler, J. E., and Davison, I. R.: High-temperature tolerance of photosynthesis in the red alga
936 *Chondrus crispus,* Mar. Biol., 117(2), 327–335. https://doi.org/10.1007/BF00345678, 1993.

937 Kübler, J. E., and Dudgeon, S. R.: Predicting effects of ocean acidification and warming on algae
938 lacking carbon concentrating mechanisms, *PLoS One,* 10 (7),
939 https://doi.org/10.1371/journal.pone.0132806, 2015.

940 Lapointe, B. E., and Duke, C. S.: Biochemical strategies for growth of *Gracilaria tikvahiae*
941 (Rhodophyta) in relation to light intensity and nitrogen availability, J. Phycol., 20(4), 488–495.
942 https://doi.org/10.1111/j.0022-3646.1984.00488.x, 1984.

943 Littler, M. M., and Littler, D. S.: The evolution of thallus form and survival strategies in benthic
944 marine macroalgae: field and laboratory tests of a functional form model, Am Nat., 116, 25–44,
945 1980.

946 Littler, M. M., and Arnold, K. E.: Primary productivity of marine macroalgal functional-form groups
947 from south-western North America, J. Phycol., 18, 307–311, https://doi.org/10.1111/j.1529-
948 8817.1982.tb03188.x, 1982.

949 Lobban, C. S., Harrison, P. J., and Harrison, P. J.: Seaweed ecology and physiology. Cambridge
950 University Press, 1994.

951 Lovelock, C. E., Reef, R., Raven, J. A., and Pandolfi, J. M.: Regional variation in $\delta^{13}C$ of coral reef
952 macroalgae, Limnol. Oceanogr., https://doi.org/10.1002/lno.11453, 2020.

953 Lluch-Cota, S. E., Aragon-Noriega, E. A., Arreguin-Sanchez, F., Aurioles-Gamboa, D., Bautista-
954 Romero, J. J., Brusca, R. C., Cervantes-Duarte, R., Cortes-Altamirano, R., Del-MonteLuna, P.,
955 Esquivel-Herrera, A., Fernández, G., Hendrickx, M. E., Hernandez-Vazquez, S., Herrera-Cervantes,
956 H., Kahru, M., Lavin, M., Lluch-Belda, D., Lluch-Cota, D. B., Lopez-Martinez, J., Marinone, S. G.,
957 Nevarez-Martinez, M. O., Ortega-Garcia, S., Palacios-Castro, E., Pares-Sierra, A., Ponce-Diaz, G.,
958 RamirezRodriguez, M., Salinas-Zavala, C. A., Schwartzlose, R. A., and Sierra-Beltran, A. P.: The
959 Gulf of California: Review of ecosystem status and sustainability challenges, Prog. Oceanogr., 73,
960 1–26, 2007.

961 Maberly, S. C., Raven, J. A. and Johnston, A. M.: Discrimination between ^{12}C and ^{13}C by marine
962 plants, *Oecologia,* 91,481–492, https://doi.org/10.1007/BF00650320, 1992.

963 Mackey, A. P., Hyndes, G. A., Carvalho, M. C., and Eyre, B. D.: Physical and biogeochemical
964 correlates of spatio-temporal variation in the $\delta^{13}C$ of marine macroalgae, Estuar. Coast. Shelf Sci.,
965 157, 7-18, https://doi.org/10.1016/j.ecss.2014.12.040, 2015.

966 Madsen, T. V., and Maberly, S. C.: High internal resistance to CO_2 uptake by submerged
967 macrophytes that use HCO_3^-: measurements in air, nitrogen and helium, Photosynth. Res., 77(2-3),
968 183–190, https://doi.org/10.1023/A:1025813515956, 2003.

969 Marinone, S. G., and Lavín, M. F.: Residual flow and mixing in the large islands' region of the
970 central Gulf of California: Nonlinear processes in geophysical fluid dynamics, Springer, Dordrechm,
971 http://doi-org-443.webvpn.fjmu.edu.cn/10.1007/978-94-010-0074-1_13, 2003.

972 Marinone, S. G.: A note on "Why does the Ballenas Channel have the coldest SST in the Gulf of
973 California?". *Geophysical research letters*, 34(2). https://doi.org/10.1029/2006GL028589, 2007.

974 Marconi, M., Giordano, M., and Raven, J. A.: Impact of taxonomy, geography and depth on the $\delta^{13}C$
975 and $\delta^{15}N$ variation in a large collection of macroalgae, J. Phycol*.,* 47, 1023–1035,
976 https://doi.org/10.1111/j.1529-8817.2011.01045.x, 2011.

977 Martínez-Díaz-de-León, A.: Upper-ocean circulation patterns in the Northern Gulf of California,
978 expressed in Ers-2 synthetic aperture radar imagery, Cienc. Mar., 27(2), 209–221,
979 https://doi.org/10.7773/cm.v27i2.465, 2001.

Martínez-Díaz-de-León, A., Pacheco-Ruíz, I., Delgadillo-Hinojosa, F., Zertuche-González, J. A., Chee-Barragán, A., Blanco-Betancourt, R., Guzmán-Calderón, J. M., and Gálvez-Telles, A.: Spatial and temporal variability of the sea surface temperature in the Ballenas-Salsipuedes Channel (central Gulf of California), J. Geophys. Res. Oceans, 111(C2), https://doi.org/10.1029/2005JC002940, 2006.

Masojidek, J., Kopecká, J., Koblížek, M., and Torzillo, G.: The xanthophyll cycle in green algae (Chlorophyta): its role in the photosynthetic apparatus, Plant Biol., 6(3), 342–349, https://doi.org/10.1055/s-2004-820884, 2004.

McConnaughey, T. A., Burdett, J., Whelan, J. F., and Paull, C. K.: Carbon isotopes in biological carbonates: respiration and photosynthesis, Geochim. Cosmochim Ac., 61(3), 611–622, https://doi.org/10.1016/S0016-7037(96)00361-4, 1997.

Mercado, J. M., De los Santos, C. B., Pérez-Lloréns, J. L., and Vergara, J. J.: Carbon isotopic fractionation in macroalgae from Cadiz Bay (Southern Spain): comparison with other bio-geographic regions, Estuar, Coast. Shelf Sci., 85, 449–458, https://doi.org/10.1016/j.ecss.2009.09.005, 2009.

Murru, M., and Sandgren, C.D.: Habitat matters for inorganic carbon acquisition in 38 species of red macroalgae (Rhodophyta) from Puget Sound, Washington, USA. J. Phycol., 40, 837–845. https://doi.org/10.1111/j.1529-8817.2004.03182.x, 2004.

Nielsen, S. L., and Jensen, K. S.: Allometric settling of maximal photosynthetic growth rate to surface/volume ratio, *Limnol. Oceanogra.*, 35(1), 177–180, https://doi.org/10.4319/lo.1990.35.1.0177, 1990.

Norris, J. N.: The marine algae of the northern Gulf of California, Ph. D. dissertation, University of California, Santa Barbara, 575 pp., 1975.

Norris, J. N.: Studies on *Gracilaria Grev*.(Gracilariaceae, Rhodophyta) from the Gulf of California, Mexico. Taxonomy of Economic Seaweeds, California Sea Grant College Program, California, I, 123-135, 1985.

Norris, J. N.: Marine algae of the northern Gulf of California: Chlorophyta and Phaoephyceae,

1007 Smithsonian contr. Bot., no. 94, https://doi.org/10.5479/si.19382812.96, 2010.

1008 Oehlert, A. M., Lamb-Wozniak, K. A., Devlin, Q. B., Mackenzie, G. J., Reijmer, J. J., and Swart, P.
1009 K.: The stable carbon isotopic composition of organic material in platform derived sediments:
1010 implications for reconstructing the global carbon cycle, Sedimentology, 59(1), 319–335,
1011 https://doi.org/10.1111/j.1365-3091.2011.01273.x, 2012.
1012 Ochoa-Izaguirre, M. J., Aguilar-Rosas, R., and Aguilar-Rosas, L. E.: Catálogo de Macroalgas de las
1013 lagunas costeras de Sinaloa, Serie Lagunas Costeras, Edited by Páez-Osuna, F., UNAM, ICMyL,
1014 México, pp 117, 2007.
1015 Ochoa-Izaguirre, M. J., and Soto-Jiménez, M. F.: Variability in nitrogen stable isotope ratios of
1016 macroalgae: consequences for the identification of nitrogen sources, J. Phycol., 51, 46–65,
1017 https://doi.org/10.1111/jpy.12250, 2015.
1018 Páez-Osuna, F., Piñón-Gimate, A., Ochoa-Izaguirre, M. J., Ruiz-Fernández, A. C., Ramírez-
1019 Reséndiz, G., and Alonso-Rodríguez, R.: Dominance patterns in macroalgal and phytoplankton
1020 biomass under different nutrient loads in subtropical coastal lagoons of the SE Gulf of California,
1021 Mar. Pollut. Bull., 77(1-2), 274-281, https://doi.org/10.1016/j.marpolbul.2013.09.048, 2013.
1022 Páez-Osuna, F., Álvarez-Borrego, S., Ruiz-Fernández, A. C., García-Hernández, J., Jara-Marini, E.,
1023 Bergés-Tiznado, M. E., Piñón-Gimate, A., Alonso-Rodríguez, R., Soto-Jiménez, M. F., Frías-
1024 Espericueta, M. G., Ruelas-Inzunza, J. R., Green-Ruíz, C. R., Osuna-Martínez, C. C., and Sánchez-
1025 Cabeza, J. A.: Environmental status of the Gulf of California: a pollution review, *Earth-Sci. Rev.*,
1026 166, 181–205, https://doi.org/10.1016/j.earscirev.2016.09.015, 2017.
1027 Pedroche, F. F., and Sentíes, A.: Ficología marina mexicana: Diversidad y Problemática actual,
1028 *Hidrobiológica*, 13(1), 23–32, 2003.
1029 Rautenberger, R., Fernández, P. A., Strittmatter, M., Heesch, S., Cornwall, C. E., Hurd, C. L., and
1030 Roleda, M. Y.: Saturating light and not increased carbon dioxide under ocean acidification drive
1031 photosynthesis and growth in *Ulva rigida* (Chlorophyta), Ecol. Evol., 5(4), 874–888,
1032 https://doi.org/10.1002/ece3.1382, 2015.

1033 Raven, J. A., Johnston, A. M., Kübler, J. E., Korb, R. E., McInroy, S. G., Handley, L. L., Scrimgeour,
1034 C. M., Walker, D. I., Beardall, J., Clayton, M. N., Vanderklift, M., Fredriksen, S., and Dunton, K.
1035 H.: Seaweeds in cold seas: evolution and carbon acquisition, Ann. Bot., 90, 525–536.
1036 https://doi.org/10.1093/aob/mcf171, 2002a.

Raven, J. A., Johnshton, A. M., Kübler, J. E., Korb, R. E., Mclnroy, S. G., Handley, L. L., Scrimgeour, C. M., Walker, D. I., Beardall, J., Vanderklift, M., Fredriksen, S., and Dunton, K. H.: Mechanistic interpretation of carbon isotope discrimination by marine macroalgae and seagrasses, Funct. Plant Biol., 29:355–378, https://doi.org/10.1071/PP01201, 2002b.

Raven, J. A., Ball, L. A., Beardall, J., Giordano, M., and Maberly, S. C.: Algae lacking carbon-concentrating mechanisms, Can. J. Bot., 83(7), 879–890, https://doi.org/10.1139/b05-074, 2005.

Raven, J. A., and Beardall, J.: The ins and outs of CO_2, J. Exp. Bot., *67*(1), 1–13, https://doi.org/10.1093/jxb/erv451, 2016.

Roberts, K., Granum, E., Leegood, R. C., and Raven, J. A.: C3 and C4 pathways of photosynthetic carbon assimilation in marine diatoms are under genetic, not environmental control, Plant Physiol., 145(1), 230–235, https://doi.org/10.1104/pp.107.102616, 2007.

Roden, G. I.: Oceanographic and meteorological aspects of the Gulf of California, 1958.

Roden, G. I., and Groves, G. W.: Recent oceanographic investigations in the Gulf of California, J. Mar. Res., 18(1), 10–35, 1959.

Roden, G. I., and Emilsson, L.: Physical oceanography of the Gulf of California. Simposium Golfo de California, Universidad Nacional Autónoma de México, Mazatlán, Sinaloa, México, 1979.

Rusnak, G. A., Fisher, R. L., and Shepard, F. P.: Bathymetry and faults of Gulf of California. In: van Andel, Tj. H. and G.G. Shor, Jr. (editors), Marine Geology of the Gulf of California: A symposium, *AAPG Memoir*, 3, 59–75, https://doi.org/10.1306/M3359C3, 1964.

Sand-Jensen, K., and Gordon, D.: Differential ability of marine and freshwater macrophytes to utilize HCO_3^- and CO_2, Mar. Biol., 80, 247–253, https://doi.org/10.1111/j.1469-8137.1981.tb03198.x, 1984.

Sanford, L. P., and Crawford, S. M.: Mass transfer versus kinetic control of uptake across solid-water boundaries, Limnol. Oceanogr., 45, 1180−1186, https://doi.org/10.4319/lo.2000.45.5.1180, 2000.

Santamaría-del-Angel, E., Alvarez-Borrego, S., and Müller-Karger, F. E.: Gulf of California biogeographic regions based on coastal zone color scanner imagery, J. Geophys. Res., 99, 7411–7421, https://doi.org/10.1029/93JC02154, 1994.

Santos, G. M., Ferguson, J., Acaylar, K., Johnson, K. R., Griffin, S., and Druffel, E.: $\Delta^{14}C$ and $\delta^{13}C$ of seawater DIC as tracers of coastal upwelling: A 5-year time series from Southern California, Radiocarbon, 53(4), 669-677, https://doi.org/10.1017/S0033822200039126, 2011.

Setchell, W., and Gardner, N.: The marine algae of the Pacific Coast of North America. Part II Chlorophyceae, Univ. Calif. Publ. Bot., 8, 139–374, https://doi.org/10.5962/bhl.title.5719, 1920.

Setchell, W., and Gardner, N.: The marine algae: Expedition of the California Academy of Sciences to the Gulf of California in 1921, Proc. Calif. Acad. Sci., *4th series,* 12(29), 695–949, 1924.

Sharkey, T. D., and Berry, J. A.: Carbon isotope fractionation of algae as influenced by an inducible CO_2 concentrating mechanism. Inorganic carbon uptake by aquatic photosynthetic organisms, 1985.

Stepien, C. C.: Impacts of geography, taxonomy and functional group on inorganic carbon use patterns in marine macrophytes, J. Ecol., 103(6), 1372–1383, https://doi.org/10.1111/1365-2745.12451, 2015.

Teichberg, M., Fox, S. E., Olsen, Y. S., Valiela, I., Martinetto, P., Iribarne, O., Muto, E. Y., Petti, M. A., Cobrisier, T. N., Soto-Jiménez, M., Páez-Osuna, F., Castro, P., Freitas, H., Zitelli, A., Cardinaletti, M. and Tagliapietra, D.: Eutrophication and macroalgal blooms in temperate and tropical coastal waters: nutrient enrichment experiments with Ulva spp., Global Change Biology, 16(9), 2624-2637, https://doi.org/10.1111/j.1365-2486.2009.02108.x, 2010.

Valiela, I., Liu, D., Lloret, J., Chenoweth, K., and Hanacek, D.: Stable isotopic evidence of nitrogen sources and C4 metabolism driving the world's largest macroalgal green tides in the Yellow Sea, Sci. Rep., 8(1), 1–12, https://doi.org/10.1038/s41598-018-35309-3, 2018.

Vásquez-Elizondo, R. M., and Enríquez, S.: Light absorption in coralline algae (Rhodophyta): a morphological and functional approach to understanding species distribution in a coral reef lagoon, Front. Mar. Sci., 4, 297, https://doi.org/10.3389/fmars.2017.00297, 2017.

Vásquez-Elizondo, R. M., Legaria-Moreno, Pérez-Castro, M.A., Krämer, W. E., Scheufen, T.,

1090 Iglesias-Prieto, R., and Enríquez, S.: Absorptance determinations on multicellular tissues,
1091 Photosynth, Res., 132, 311–324, https://doi.org/10.1007/s11120-017-0395-6, 2017.

1092 Velasco-Fuentes, O. V., and Marinone, S. G.: A numerical study of the Lagrangian circulation in the
1093 Gulf of California, J. Mar. Syst., 22(1), 1–12. https://doi.org/10.1016/S0924-7963(98)00097-9,
1094 1999.

1095 Young, E. B., and Beardall, J.: Modulation of photosynthesis and inorganic carbon acquisition in a
1096 marine microalga by nitrogen, iron, and light availability, Can. J. Bot., 83(7), 917–928,
1097 https://doi.org/10.1139/b05-081, 2005.

1098 Young, J. N., Heureux, A. M., Sharwood, R. E., Rickaby, R. E., Morel, F. M., and Whitney, S. M.:
1099 Large variation in the Rubisco kinetics of diatoms reveals diversity among their carbon-
1100 concentrating mechanisms, J. Exp. Bot., 67(11), 3445–3456, https://doi.org/10.1093/jxb/erw163,
1101 2016.

1102 Xu, J., Fan, X., Zhang, X., Xu, D., Mou, S., Cao, S., Zheng, Z., Miao, J., Ye, N.: Evidence of
1103 coexistence of C3 and C4 photosynthetic pathways in a green-tide-forming alga, *Ulva prolifera,*
1104 *PloS one*, 7(5), e37438, https://doi.org/10.1371/journal.pone.0037438, 2012.

1105 Xu, J., Zhang, X., Ye, N., Zheng, Z., Mou, S., Dong, M., Xu, D. and Miao, J.: Activities of principal
1106 photosynthetic enzymes in green macroalga *Ulva linza*: functional implication of C4 pathway in CO_2
1107 assimilation, Sci. China Life Sci., 56(6), 571–580, https://doi.org/10.1007/s11427-013-4489-x,
1108 2013.

1109 Wefer, G., and Berger, W. H.: Stable isotope composition of benthic calcareous algae from Bermuda,
1110 J. Sediment. Res., 51(2), 459–465, https://doi.org/10.1306/212F7CAC-2B24-11D7-
1111 8648000102C1865D, 1981.

1112 Wilkinson T. E., Wiken, J., Bezaury-Creel, T., Hourigan, T., Agardy, H., Herrmann, L., Janishevski,
1113 C. Madden, L. Morgan and M. Padilla.: Marine Ecoregions of North America. CEC, Montreal,
1114 Canada, 2009.

1115 Zabaleta, E., Martin, M. V., and Braun, H. P.: A basal carbon concentrating mechanism in plants?,
1116 Plant Sci., 187, 97–104, https://doi.org/10.1016/j.plantsci.2012.02.001, 2012.

Zeebe, R. E., and Wolf-Gladrow, D.: CO_2 in seawater: equilibrium, kinetics, isotopes (No. 65) Gulf Professional Publishing, 2001.

Zeitzschel, B.: Primary productivity in the Gulf of California, Mar. Biol., 3(3), 201–207, https://doi.org/10.1007/BF00360952, 1969.

Zou, D., Xia, J., and Yang, Y.: Photosynthetic use of exogenous inorganic carbon in the agarophyte *Gracilaria lemaneiformis* (Rhodophyta), Aquac, 237, 421-431, https://doi.org/10.1016/j.aquaculture.2004.04.020, 2004.

Figure captions

Fig. 1. Sites collection along the continental (C1-C3) and peninsula (P1-P3) Gulf of California coastlines (A), range of environmental factors supporting or limiting the life processes for the macroalgal communities within a habitat (B), and inserted Table with the features and environmental conditions in the diverse habitats in the GC bioregions that delimits the macroalgal community's zonation.

Fig. 2. Variability of $\delta^{13}C$ values for specimens of different macroalgae genera collected along GC coastlines classified by taxon: (A) Chlorophyta, (B) Ochrophyta and (C) Rhodophyta. Shaded background represents the cutoff limits for using CO_2 Only users and HCO_3^- only users, respectively, according to Raven et al., (2002).

Fig. 3. Variability of $\delta^{13}C$ values for the genus collected along coastline of the Gulf of California according to their taxon: (A) Chlorophyta, (B) Ochrophyta and (C) Rhodophyta. Genus with n=1 is not shown, and genus n=2 was not considered to the statistical comparison. Different letters indicate significant differences ($P<0.05$): a>b>c>d>e. Shaded background represent the cutoff limits for using CO2 Only users and HCO3- only users, respectively, according to Raven et al., (2002). For Chlorophyta: Bry= *Bryopsis*, Cau=*Caulerpa*, Cha= *Chaetomorpha*, Cla= *Cladophora*, Cod= *Codium*, Phy= *Phyllodictyon*, Str= *Struveopsis*, Ulv=*Ulva.* Phaeophyta: Col= *Colpomenia*, Dic= *Dictyota*, Ect= *Ectocarpus*, End= *Endarachne*, Hyd= *Hydroclathatrus*, Pad= *Padina*, Ros= *Rosenvigea*, Sar= *Sargassum*, Spa= *Spatoglossum*, Zon= *zonaria.* Rhodophyta: Aca: *Acantophora*, anf: *Anfeltiopsis*, Amp= *Amphiroa*, Cen= *Centroceras*, Cer[1]= *Ceramium*, Cer[2] = *Ceratodictyon*, Cho[1]= *Chondracanthus*, Cho[2]= *Chondria*, Das= *Dasya*, Dig= *Digenia*, Euc= *Euchema*, Gel= *Gelidium*, Gig= *Gigartina*, Gra[1]= *Gracilaria*, Gra[2]= *Grateloupia*, Gra[3]= *Gracilariopsis*, Gym=

Gymnogongrus, Hal= *Halymenia*, Hyp= *Hypnea*, Jan= Jania, Lau= Laurencia, Lom= *Lomentaria*, Neo= *Neosiphonia*, Pol= *Polysiphonia*, Pri= *Prionitis*, Rho[1]= *Rhodoglossum*, Rho[2]= *Rhodymenia*,Sch= *Schymenia*, Spy= *Spyridia*, Tac= *Tacanoosca*. Purple boxplots represent calcifying species group.

Fig. 4. Variability of $\delta^{13}C$ values for morphofunctional groups by taxa along coastline of the Gulf of California.

Fig. 5 Proportion of species using different DIC sources according to their carbon uptake strategies: HCO_3^- only users (CO_2 concentrating mechanism active), Users of both sources (HCO_3^- & CO_2) and CO_2 only users (non-CO_2 concentrating mechanism active) in function of coast along GC.

Fig. 6. Variability of $\delta^{13}C$ values in macroalgae specimens for the most representative genera in function of habitat features (emersion level). Green circles represent genus of Chlorophyta, Brown circles represent genus of Ochrophyta; red circles represent genus Rhodophyta and purple circles represent genus with calcifying capacity.

Fig. 7. Variability of $\delta^{13}C$ values in macroalgae specimens for the most representative genus in function of temperature (a) and pH (b) ranges in samples collected along Gulf of California coastline.

Fig. 8. Proportion of species using different DIC sources according to their carbon assimilation strategies: HCO_3^- only users (CO_2 concentrating mechanism active), Users of both sources (HCO_3^- & CO_2) and CO_2 only users (non-CO_2 concentrating mechanism active) in function of : (A) pH ranges, (B) temperature ranges and (C) salinity ranges.

1168 Fig. 9. Trends in the $\delta^{13}C$-macroalgal in specimens collected along continental (C1-C3) and

1169 peninsula (P1-P3) Gulf of California coastline in function of latitudinal gradient.

1170

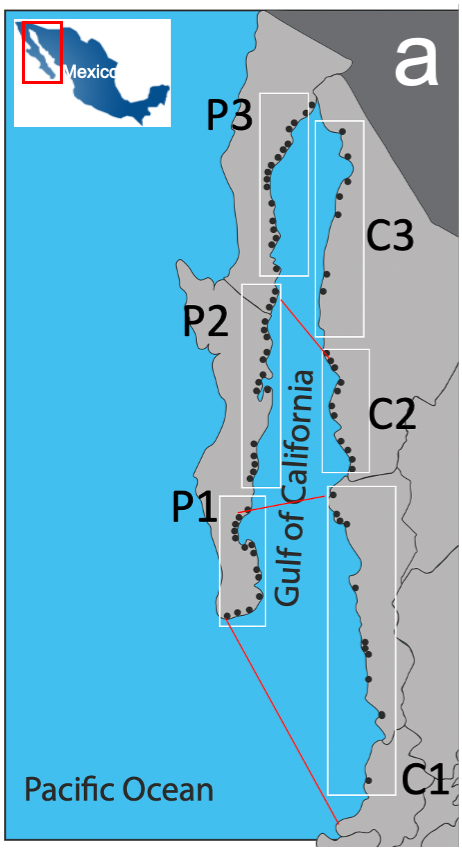

Habitats features and environmental conditions in sampling sites

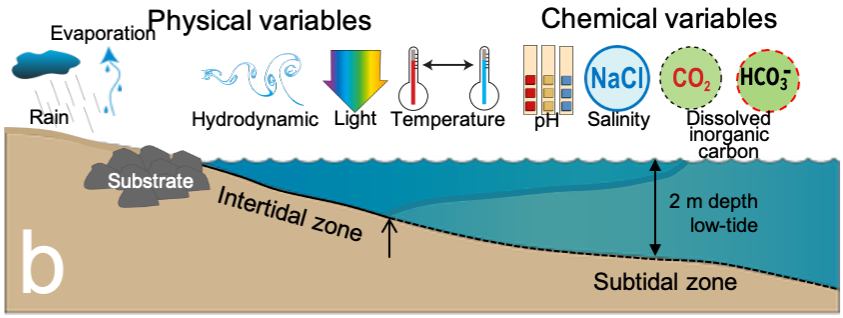

Environmental factors	Continental GC coastline			Peninsula GC coastline		
	C1	C2	C3	P1	P2	P3
Substrate at shores	Rocky and sandy-rocky	Only sandy-rocky shore	Rocky and sandy-rocky	Rocky and sandy-rocky	Rocky and sandy-rocky	Rocky and sandy-rocky
Hydrodynamic (water movement)	Slow to fast	Slow to fast	Slow to fast	Slow to fast	Slow to fast	Slow to fast
Protection level sites	Exposed and protected	Exposed and protected	Exposed and protected	Exposed and protected	Exposed and protected	Exposed and protected
Immersion level	Intertidal and subtidal	Intertidal and subtidal	Intertidal and subtidal	Intertidal and subtidal	Intertidal and subtidal	Intertidal and subtidal
pH ranges	Acid, typical and alkaline	Acid, typical and alkaline	Acid, typical and alkaline	Acid, typical and alkaline	Typical and alkaline	Acid, typical and alkaline
Temperature ranges	Typical and warmer	Colder, typical and warmer	Colder, typical and warmer	Colder, typical and warmer	Colder, typical and warmer	Colder, typical and warmer
Salinity ranges	Marine	Hypersaline, marine, estuarine	Marine	Marine	Marine	Marine

1171

1172 Fig. 1

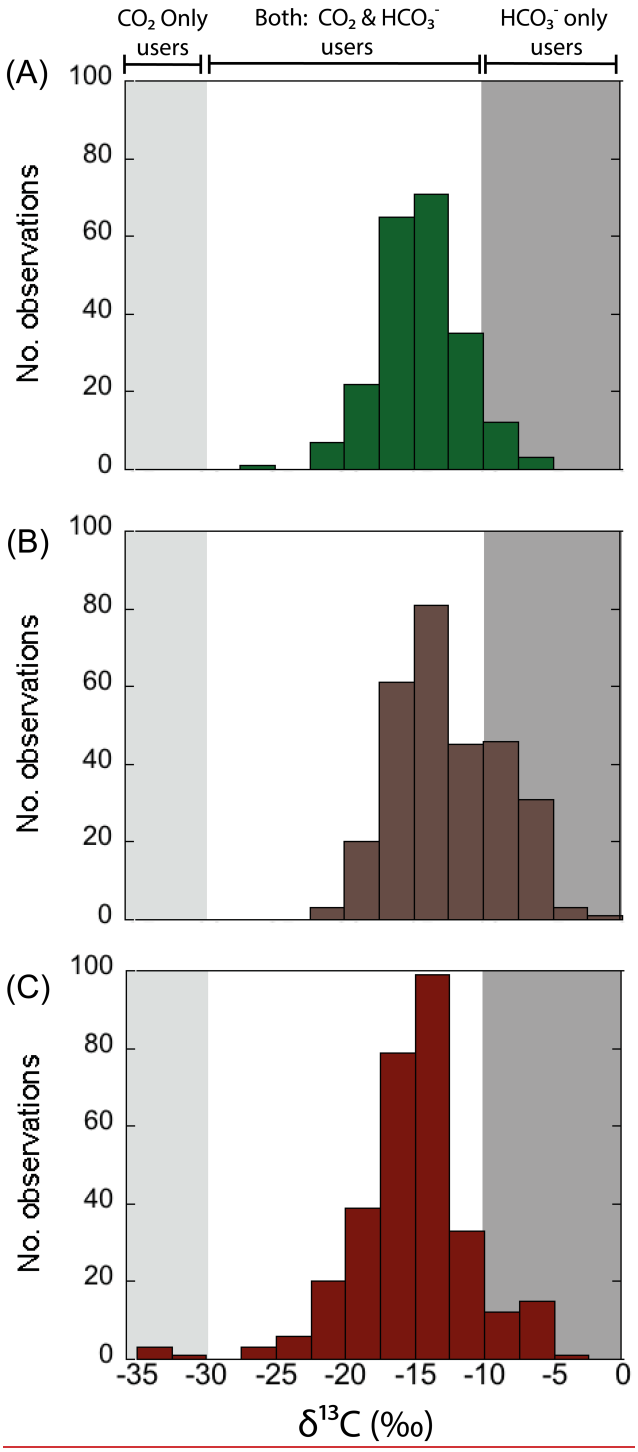
CO2 Only users
Both: CO2 & HCO3- users
HCO3- only users
(A)
(B)
(C)
No. observations
100
80
60
40
20
0
-35
-30
-25
-20
-15
-10
-5
0
δ13C (‰)

Fig 2

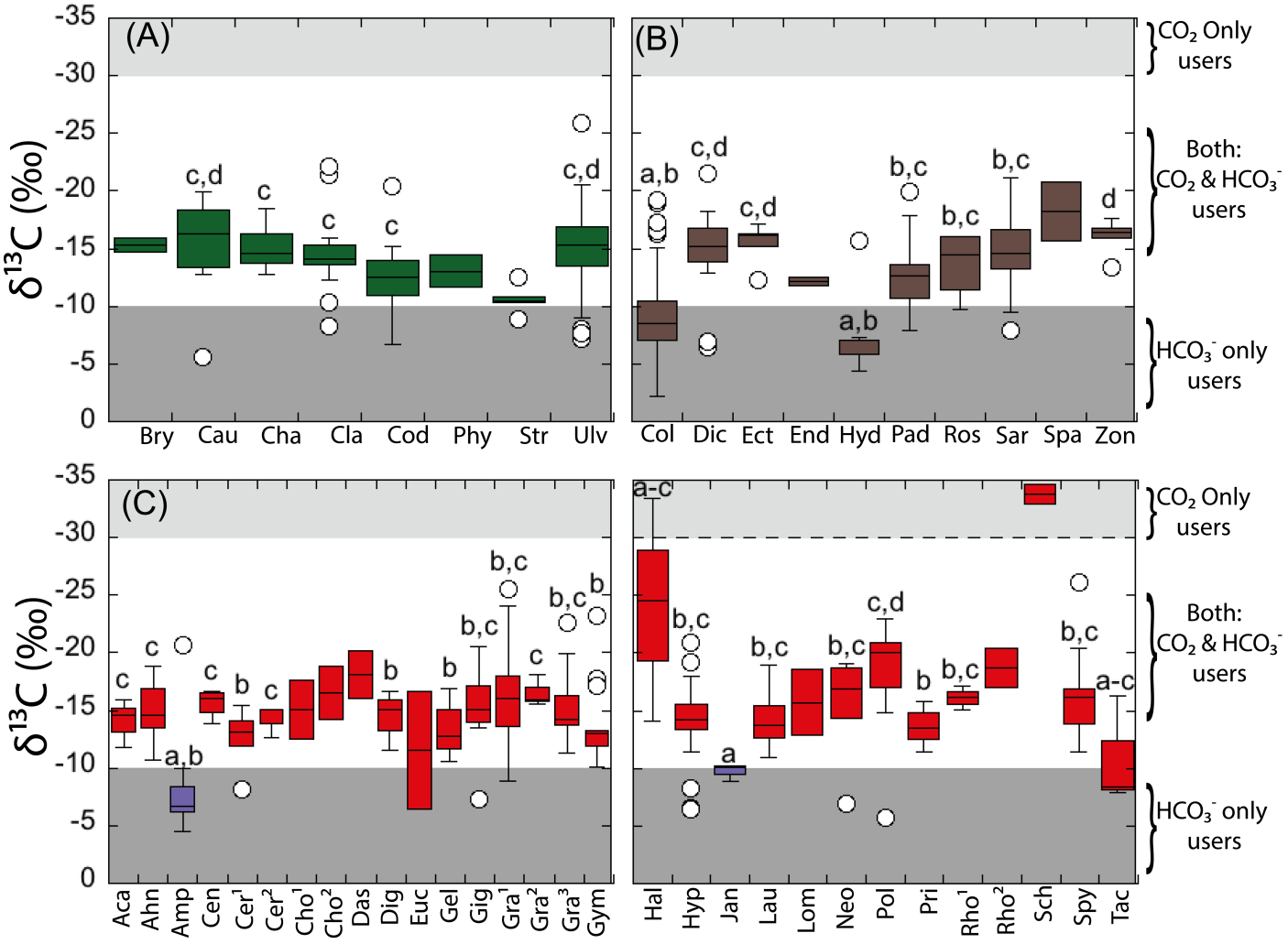
(A)
(B)
(C)
δ13C (‰)
-35
-30
-25
-20
-15
-10
-5
0
CO2 Only users
Both: CO2 & HCO3- users
HCO3- only users
Bry Cau Cha Cla Cod Phy Str Ulv
Col Dic Ect End Hyd Pad Ros Sar Spa Zon
Aca Ahn Amp Cen Cer1 Cer2 Cho1 Cho2 Das Dig Euc Gel Gig Gra1 Gra2 Gra3 Gym
Hal Hyp Jan Lau Lom Neo Pol Pri Rho1 Rho2 Sch Spy Tac

Fig 3

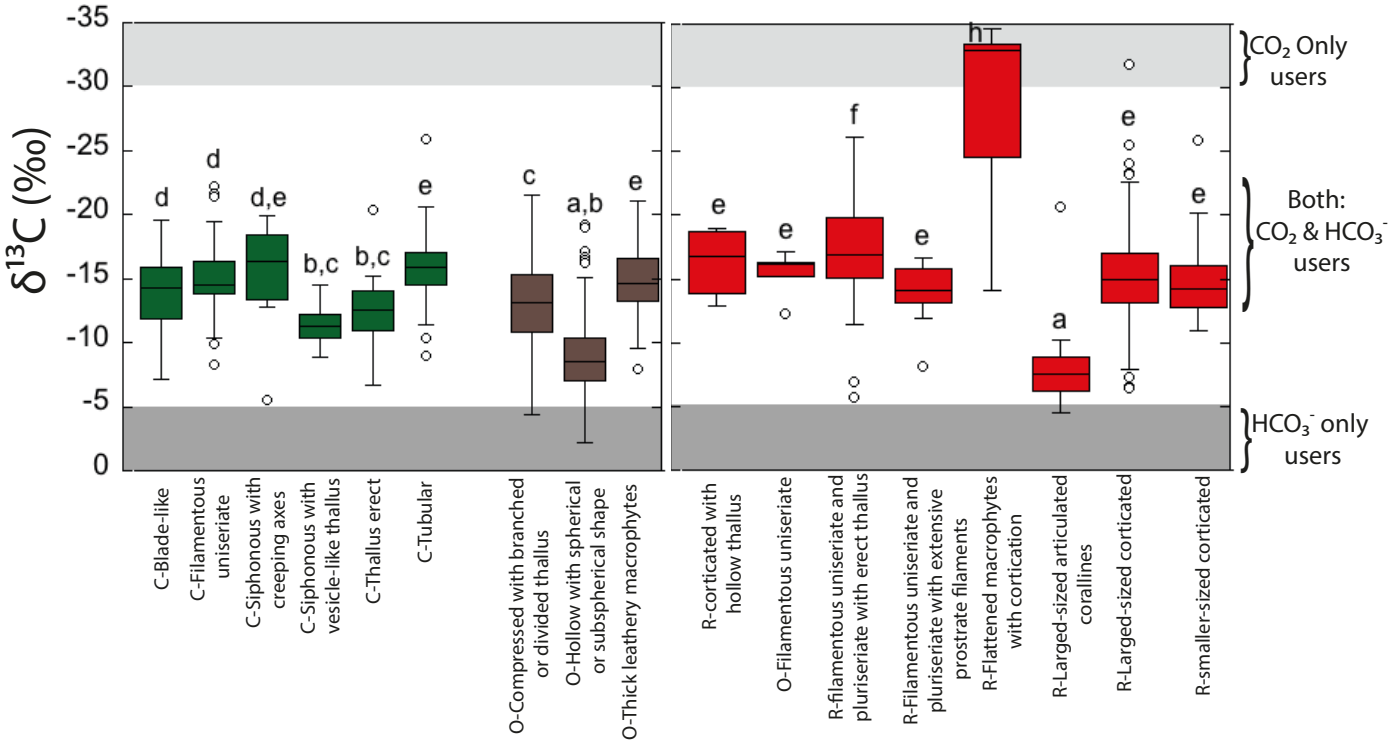

1180

1181 **Fig 4**

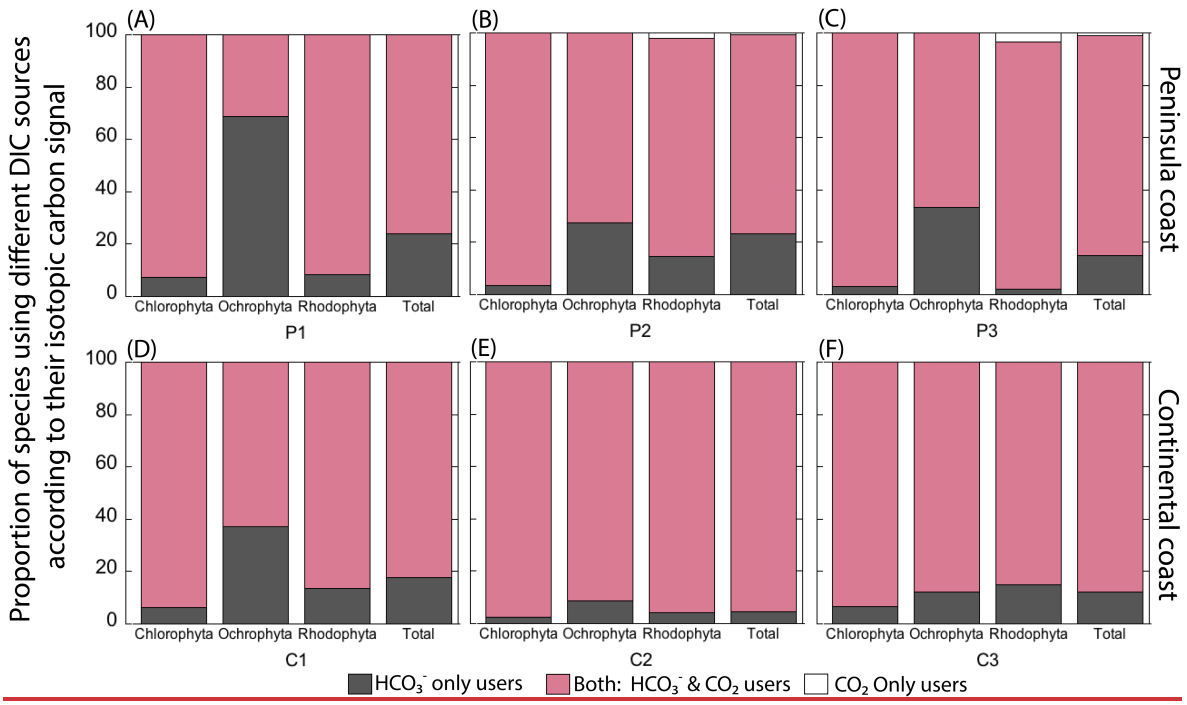
Proportion of species using different DIC sources according to their isotopic carbon signal
(A)
(B)
(C)
(D)
(E)
(F)
100
80
60
40
20
0
Chlorophyta Ochrophyta Rhodophyta Total
P1
P2
P3
C1
C2
C3
Peninsula coast
Continental coast
HCO3- only users
Both: HCO3- & CO2 users
CO2 Only users

Fig 5

1184

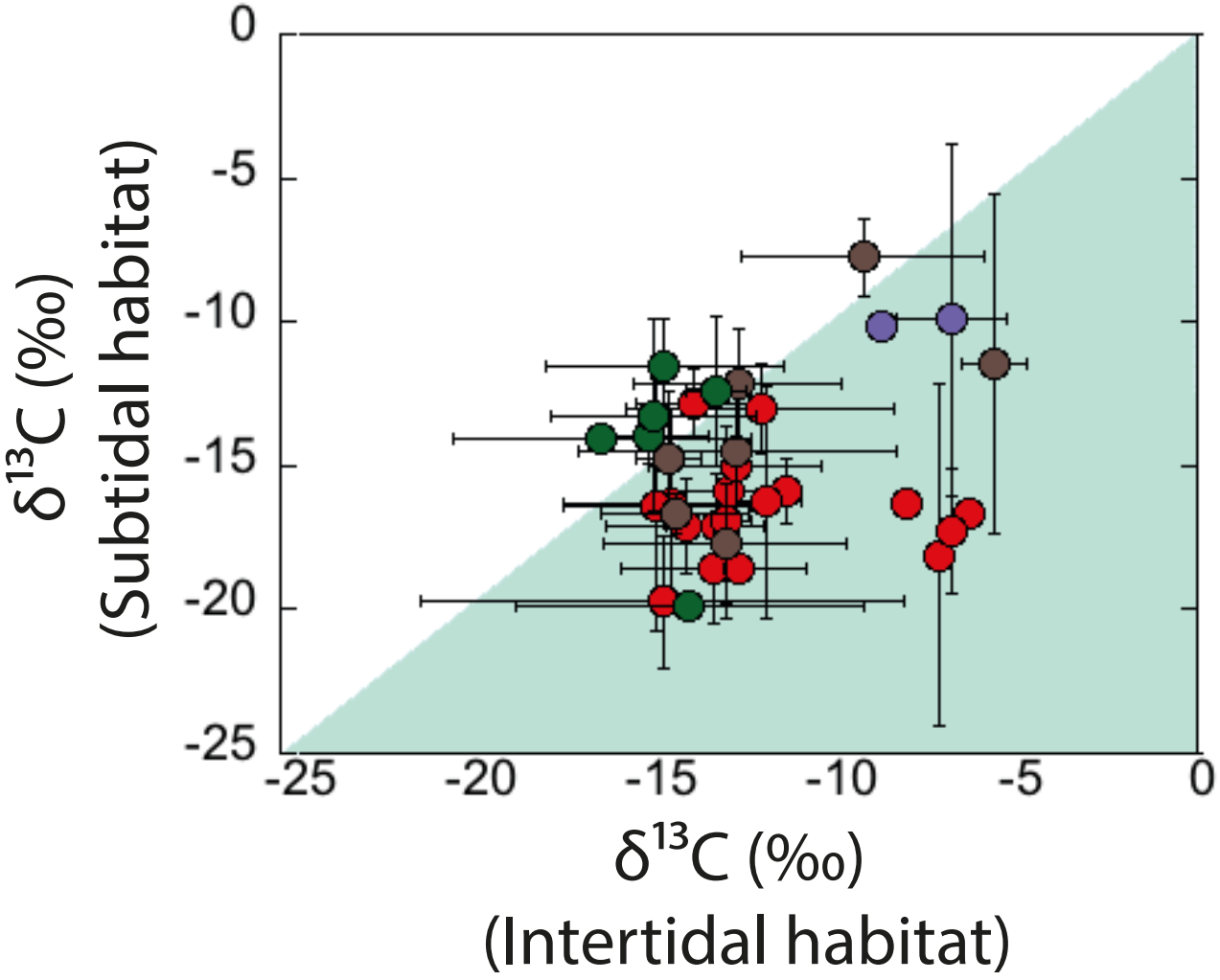

1185

1186 **Fig 6**

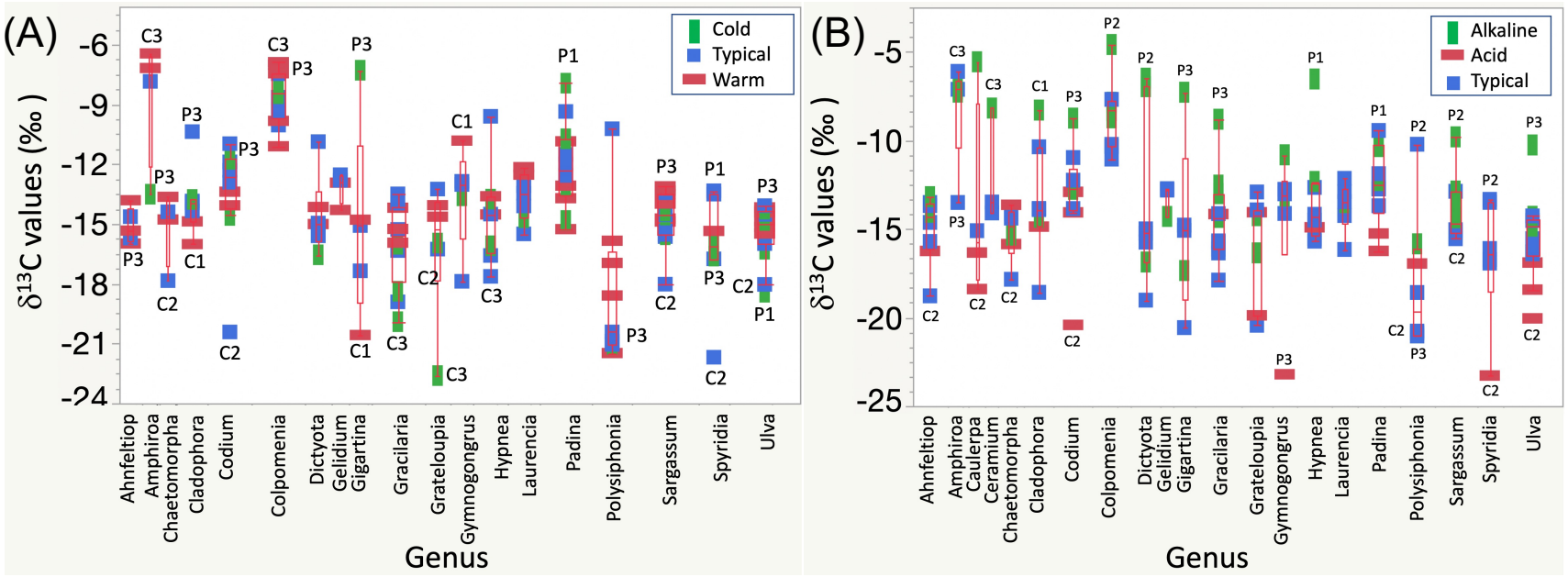

1187

1188 **Fig 7**

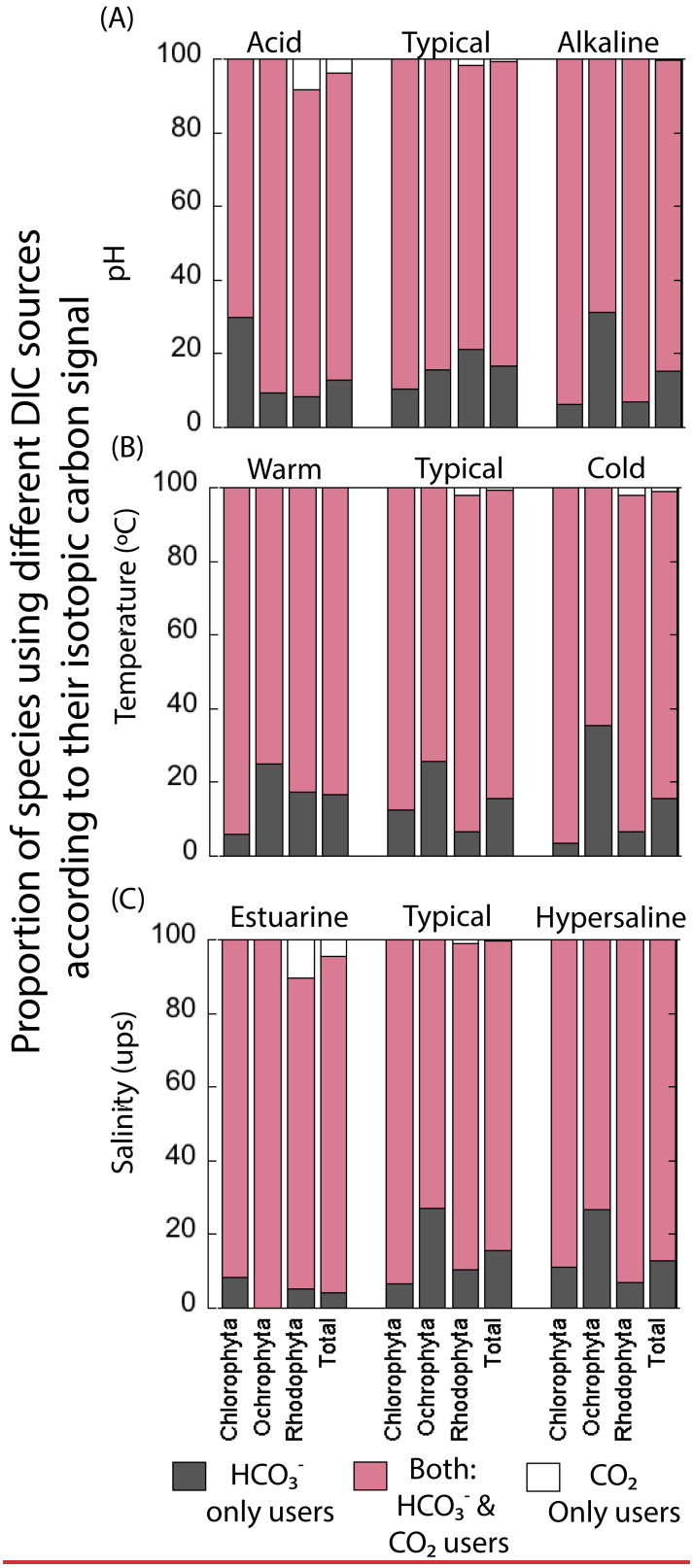

1189

1190 **Fig 8**

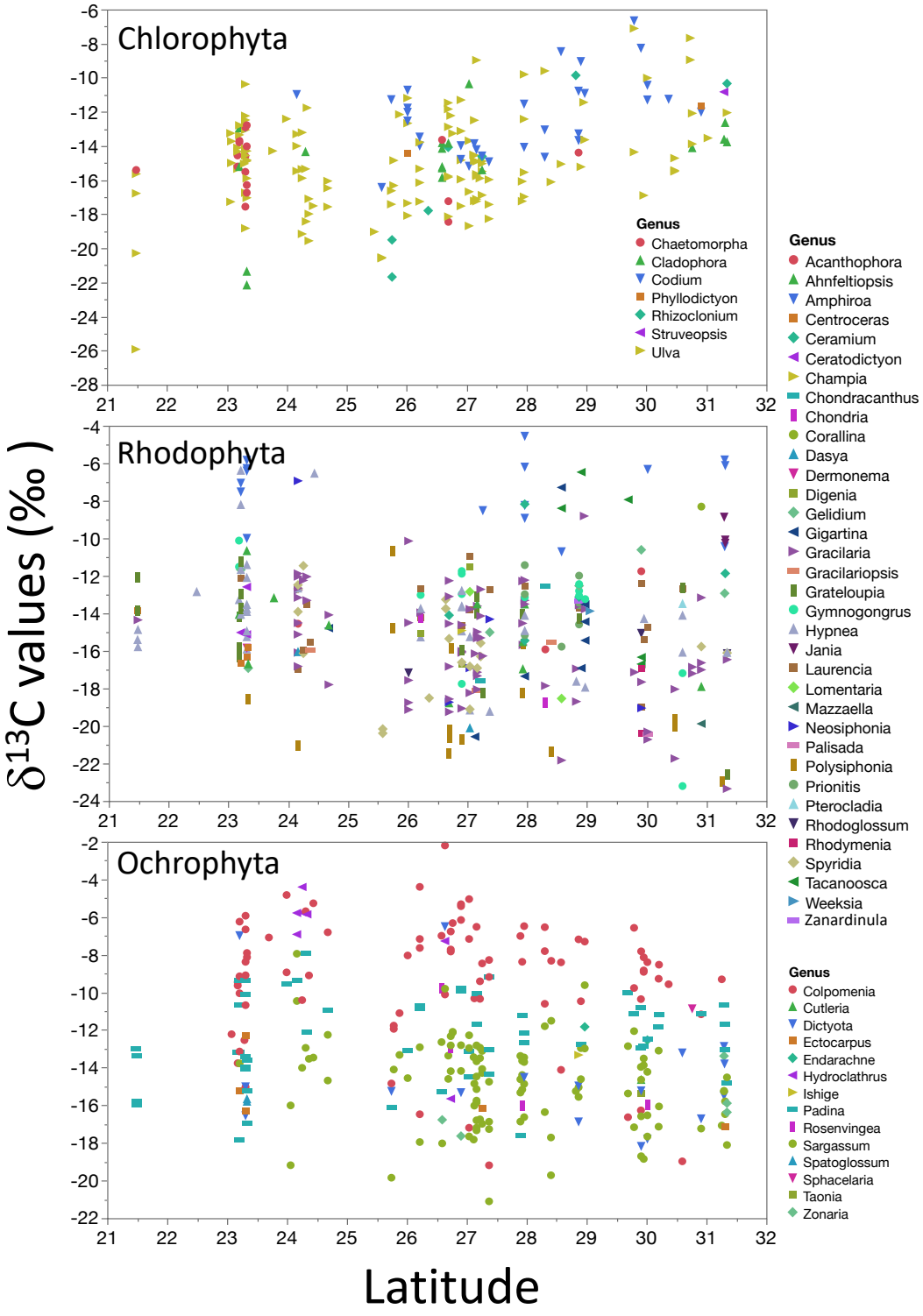

1191

1192 **Fig. 9**

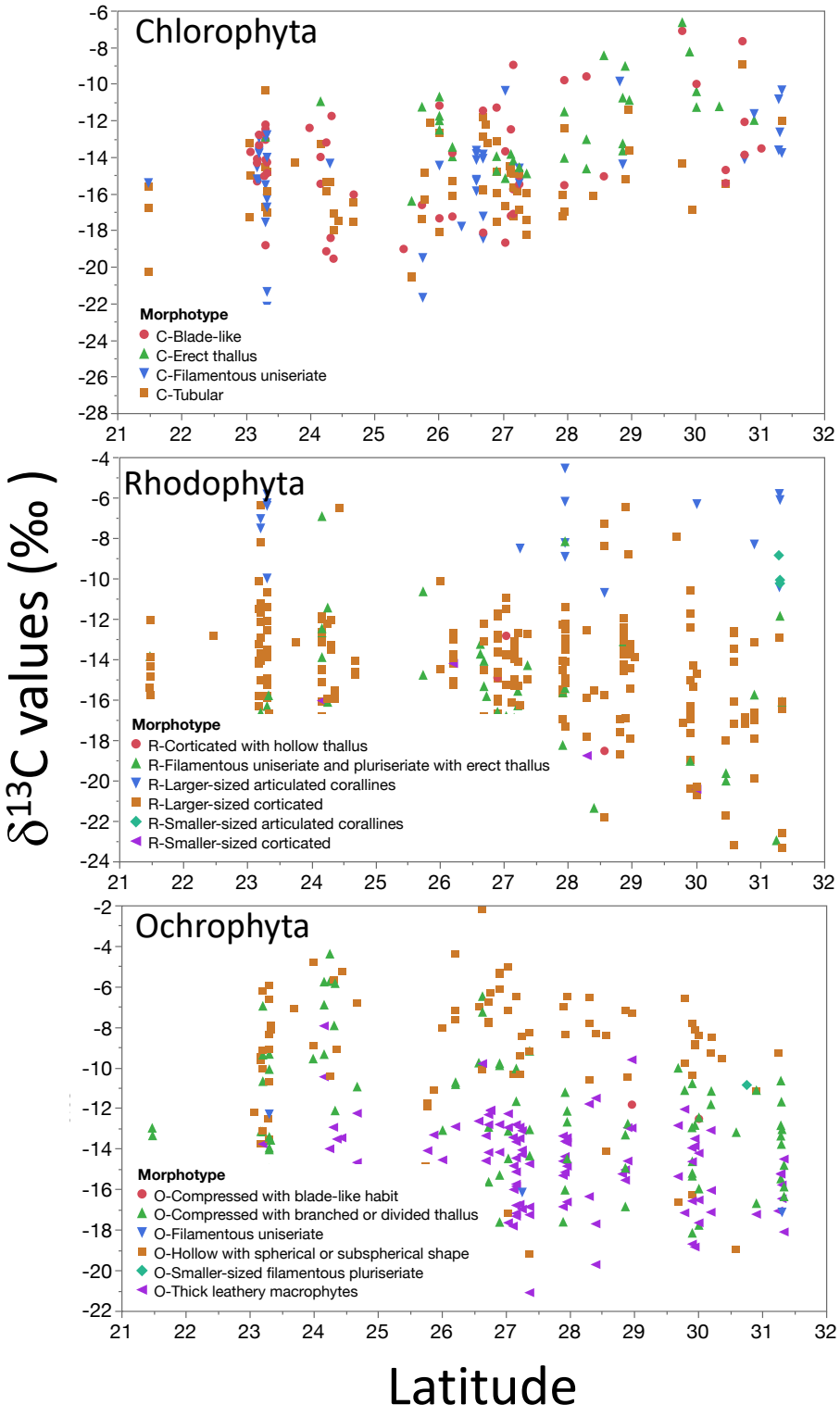

1193

1194 **Fig. 10**

Table 1. Carbon isotopic composition (‰) in species of Phyla Chlorophyta collected along Gulf of California coastlines.

Species (n composite samples)	$\delta^{13}C \pm SD$ (Min to Max, ‰)
Chaetomorpha sp. (3)	-13.7±0.8 (-14.6 to -12.9)
C. antennina (10)	-14.6±1.1 (-16.3 to -12.8)
C. linum (5)	-16.8±1.6 (-18.5 to -14.6)
Codium sp. (5)	-11.6±3.0 (-14.1 to-6.7)
C. amplivesiculatum (8)	-14.4±2.7 (-20.4 to -11.3)
C. brandegeei (7)	-11.8±1.2 (-13.7 to -10.4)
C. fragile (4)	-13.0±2.7 (-14.8 to -9.0)
C. simulans (9)	-11.4±2.2 (-14.9 to -8.3)
Ulva sp. (12)	-14.0±3.9 (-19.2 to -7.1
U. acanthophora (25)	-15.8±1.7 (-18.3 to -11.4)
U. clathrata (8)	-16.4± 2.0 (-20.5 to -14.5)
U. compressa (4)	-17.8±2.4 (-20.6 to -15.4)
U. flexuosa (13)	-16.0±3.7 (-25.9 to -10.4)
U. intestinalis (16)	-15.3±2.5 (-20.3 to -8.9)
U. lactuca (31)	-14.1±3.1 (-19.6 to -7.7)
U. linza (6)	-15.6±2.4 (-19.4 to -13.2)
U. lobata (5)	-13.2±1.9 (-15.3 to -11.1)
U. prolifera (3)	-14.2±1.8 (-15.5 to -12.2)

1195

Table 2. Carbon isotopic composition (‰) in species of Phyla Ochrophyta collected along Gulf of California coastlines.

Species (n composite samples)	$\delta^{13}C \pm SD$ (Min to Max, ‰)
Colpomenia sp. (11)	-11.0±3.7 (-19.0 to -5.4)
C. ramosa (4)	-11.4±2.6 (-13.8 to-7.8)
C. sinuosa (7)	-10.2±3.0 (-16.3 to -7.2)
C. tuberculata (64)	-8.7±3.2 (-19.2 to -2.2)
Padina sp. (15)	-11.1±1.5 (-13.1 to-7.9)
P. crispata (3)	-11.3±1.7 (-12.5 to -10.1)
P. durvillaei (36)	-13.2±2.6 (-20.0 to -9.2)
Sargassum sp. (34)	-14.3±2.4 (-18.7 to -8.0)
S. herporhizum (7)	-13.7±1.6 (-16.6 to -11.5)
S. horridum (12)	-15.5±2.9 (-19.7 to-9.5)
S. johnstonii (10)	-15.4±2.0 (-17.7 to -11.8)
S. lapazeanum (7)	-14.49±1.59 (-17.2 to -12.8)
S. sinicola (31)	-15.1±2.4 (-21.1 to -12.1)

1196

1197 Table 3. Carbon isotopic composition (‰) in species of Phyla Rhodophyta collected along Gulf of
1198 California coastlines.

Species (n composite samples)	$\delta^{13}C \pm SD$ (Min to Max, ‰)
Gracilaria sp. (18)	-15.5±2.4 (-21.8 to -12.2)
Gracilaria sp.2 (3)	-14.4±3.7 (-18.7 to -12.3)
G. crispata (7)	-15.1±3.0 (-19.1 to -10.1)
G. pacifica (6)	-16.5±1.6 (-18.6 to -13.6)
G. spinigera (3)	-14.9±3.8 (-17.7 to -12.2)
G. subsecundata (8)	-15.9±2.8 (-20.3 to -12.8)
G. tepocensis (3)	-15.1±1.9 (-17.0 to -13.2)
G. textorii (4)	-16.2±2.6 (-18.1 to -14.3)
G. turgida (5)	-15.3±3.6 (-20.7 to -12.0
G. vermiculophylla (16)	-15.9±3.8 (-23.4 to -8.8)
Hypnea sp. (14)	-14.9±2.6 (-20.9 to -11.4)
H. johnstonii (5)	-11.2±3.5 (-13.8 to -6.5)
H. pannosa (5)	-11.8±3.3 (-15.0 to -6.4)
H. spinella (6)	-16.4±1.8 (-19.2 to -14.9)
H. valentiae (6)	-15.2±2.3 (-19.2 to -12.7)
Laurencia sp. (8)	-12.9±1.2 (-14.7 to -10.5)
L. pacifica (8)	-14.9±2.2 (-19.0 to -12.7)
L. papillosa (3)	-15.7±0.3 (-15.9 to -15.6)
Spyrida sp. (5)	-17.1±1.12 (-19.1 to -16.1)
S. filamentosa (14)	-15.9±3.8 (-26.2 to -11.5)

1199

1200

1201

Table 4. Summary of the estimated regression coefficients for each simple linear regression analyses and on the constant of fitted regression models. Estimated regression coefficients includes degrees of freedom for the error (DFE), root-mean-square error (RMSE), coefficients of determination (R^2) and the adjusted R^2 statistics, Mallow's Cp criterion (Cp), Akaike Information Criterion (AIC), Bayesian Information Criterion (BIC) minimum, F Ratio test, and p-value for the test (Prob > F). Models information includes value of the constant a ($\delta^{13}C$, ‰), standard error (SE), t ratio and Prob > |t| (values * are significant).

	Estimated regression coefficients									Model constant (a)			
Independent variables	**DFE**	**RMSE**	**R^2**	**Adjust R^2**	**Cp**	**AICc**	**BIC**	**F ratio**	**Prob > F**	**$\delta^{13}C$ (‰)**	**SE**	**t ratio**	**Prob > |t|**
Inherent macroalgae properties													
Phyla	806	3.66	0.08	0.07	3	4,401	4,420	33.1	<.0001**	-13.98	0.13	-107.4	<.0001**
Morphofunctional	788	3.10	0.35	0.34	21	4,149	4,251	21.6	<.0001**	-14.21	0.35	-40.80	<.0001**
Genus	746	2.92	0.46	0.41	63	4,104	4,393	10.1	<.0001**	-14.71	0.23	-62.64	<.0001*
Species	641	2.79	0.57	0.46	168	4,195	4,898	5.2	<.0001**	-14.60	0.16	-93.22	<.0001**
Biogeographical collection zone													
GC coastline	807	3.79	0.01	0.01	2	4,456	4,470	7.4	0.0067*	-13.97	0.13	-104.5	<.0001**
Coastal sector	803	3.73	0.05	0.04	6	4,433	4,465	7.9	<.0001*	-14.12	0.16	-90.85	<.0001**
Latitude	807	3.80	0.00	0.00	2	4,462	4,476	1.5	0.23	-12.25	1.41	-8.71	<.0001**
Longitude	807	3.81	0.00	-0.00	2	4,463	4,477	0.1	0.80	-15.44	5.83	-2.65	0.0082*
Habitat features													
Substrate	807	3.80	0.00	0.00	2	4,460	4,474	3.2	0.08	-13.82	0.15	-92.06	<.0001*
Hydrodynamic	807	3.80	0.00	0.00	2	4,462	4,476	1.3	0.26	-13.88	0.15	-95.00	<.0001**
Emersion level	807	3.69	0.06	0.06	2	4,412	4,427	52.2	<.0001**	-14.05	0.13	-107.6	<.0001**
Environmental conditions													
Temperature	802	3.70	0.01	0.01	2	4,390	4,404	5.4	0.0207*	-16.11	0.96	-16.78	<.0001*
pH	807	3.73	0.04	0.04	2	4,430	4,444	33.4	<.0001**	-32.45	3.21	-10.13	<.0001**
Salinity	806	3.80	0.00	-0.00	2	4,456	4,470	0.9	0.34	-15.77	1.91	-8.27	<.0001**

*p<0.05, **p<0.0001

Table 5. Summary of the estimated regression coefficients for each multivariate linear regression analyses and on their constant of fitted regression models performed in individuals binned by genus. Estimated regression coefficients include degrees of freedom for the error (DFE), root-mean-square error (RMSE), coefficients of determination (R^2) and the adjusted R^2 statistics, Mallow's Cp criterion (Cp), Akaike Information Criterion (AIC), Bayesian Information Criterion (BIC) minimum, F Ratio test, and p-value for the test (Prob > F). Model information includes value of the constant a ($\delta^{13}C$, ‰), standard error (SE), t ratio and Prob > |t| (values * are significant).

	Estimated regression coefficients									Model constant (a)			
Independent variables	DFE	RMSE	R^2	Adjust R^2	Cp	AICc	BIC	F ratio	Prob > F	$\delta^{13}C$ (‰)	SE	t ratio	Prob > |t|
Coastal sector	652	2.78	0.57	0.47	157	4,169	4,834	20.0	<.0001*	-17.52	0.64	-27.24	<.0001*
Substrate	711	2.90	0.49	0.42	98	4,140	4,577	0.4	0.52	-16.35	0.62	-26.20	<.0001*
Hydrodynamic	714	2.87	0.50	0.43	95	4,120	4,545	0.1	0.78	-16.53	0.64	-25.95	<.0001*
Emersion level	713	2.77	0.53	0.47	96	4,060	4,489	153.0	<.0001*	-16.65	0.60	-27.85	<.0001*
Temperature	695	2.81	0.50	0.43	109	4,083	4,564	98.4	<.0001*	-14.60	0.92	-15.91	<.0001*
Temperature ranges	686	2.87	0.49	0.40	118	4,128	4,645	97.7	<.0001*	-12.91	0.40	-31.97	<.0001*
pH	701	2.86	0.51	0.43	108	4,134	4,611	156.6	<.0001*	-28.57	2.69	-10.64	<.0001*
pH ranges	697	2.67	0.57	0.51	112	4,028	4,522	152.2	<.0001*	-16.39	0.58	-28.05	<.0001*
Salinity	697	2.89	0.50	0.42	111	4,151	4,640	162.2	<.0001*	-17.75	1.63	-10.88	<.0001*
Salinity ranges	721	2.91	0.47	0.41	86	4,117	4,504	167.8	<.0001*	-17.64	0.74	-23.68	<.0001*

Table 6. Summary of the estimated regression coefficients for each multivariate linear regression analyses and on their constant of fitted regression models performed in individuals binned by coastline sector and genus. Estimated regression coefficients include degrees of freedom for the error (DFE), root-mean-square error (RMSE), coefficients of determination (R^2) and the adjusted R^2 statistics, Mallow's Cp criterion (Cp), Akaike Information Criterion (AIC), Bayesian Information Criterion (BIC) minimum, F Ratio test, and p-value for the test (Prob > F). Model information includes value of the constant a ($\delta^{13}C$, ‰), standard error (SE), t ratio and Prob > |t| (values * are significant).

	Estimated regression coefficients									Model constant (a)			
Independent variables	DFE	RMSE	R^2	Adjust R^2	Cp	AICc	BIC	F ratio	Prob > F	$\delta^{13}C$ (‰)	SE	t ratio	Prob > |t|
Substrate	590	2.76	0.62	0.47	219	4,287	5,155	15.8	<.0001*	-17.08	0.66	-25.72	<.0001*
Hydrodynamic	592	2.73	0.62	0.49	217	4,266	5,128	18.6	<.0001*	-17.18	0.67	-25.70	<.0001*
Protection level	590	2.75	0.62	0.48	219	4,285	5,153	20.0	<.0001*	-17.51	0.64	-27.22	<.0001*
Emersion level	603	2.69	0.63	0.50	206	4,217	5,045	18.6	<.0001*	-17.47	0.64	-27.49	<.0001*
Temperature ranges	569	2.74	0.61	0.46	235	4,293	5,202	28.0	<.0001*	-13.73	0.45	-30.32	<.0001*
pH ranges	580	2.50	0.69	0.57	229	4,155	5,051	9.7	0.0019*	-16.88	0.62	-27.15	<.0001*
Salinity ranges	631	2.76	0.58	0.47	176	4,183	4,913	21.2	<.0001*	-18.30	0.79	-23.05	<.0001*

1234 Table 7. Summary of the estimated regression coefficients for each multivariate linear regression
1235 analyses and on their constant of fitted regression models performed in individuals binned in
1236 coastline sector, habitats features, environmental conditions, and Physiological performed
1237 separately by morpho-functional groups and genus. Estimated regression coefficients include
1238 degrees of freedom for the error (DFE), root-mean-square error (RMSE), coefficients of
1239 determination (R^2) and the adjusted R^2 statistics, Mallow's Cp criterion (Cp), Akaike Information
1240 Criterion (AIC), Bayesian Information Criterion (BIC) minimum, F Ratio test, and p-value for the
1241 test (Prob > F). Model information includes value of the constant a ($\delta^{13}C$, ‰), standard error (SE),
1242 t ratio and Prob > |t| (values * are significant).

	Estimated regression coefficients									Model constant (a)			
Full model	DFE	RMSE	R^2	Adjust R^2	Cp	AICc	BIC	F ratio	Prob > F	$\delta^{13}C$ (‰)	SE	t ratio	Prob > |t|
Coastline sector + Habitats features + Morphofunctional group													
I-Morpho-functional	593	2.79	0.60	0.46	216	4,301	5,160	20.8	<.0001*	-13.49	0.57	-23.52	<.0001*
Coastline sector + Environmental conditions + Morphofunctional group													
II-Morpho-functional	680	2.90	0.51	0.42	129	4,189	4,750	25.1	<.0001*	-13.42	0.54	-24.74	<.0001*
Coastline sector + Habitat features+ Genus													
I-Genus	482	2.66	0.71	0.51	327	4,565	5,655	15.8	<.0001*	-16.93	0.73	-23.27	<.0001*
Coastline sector + Environmental conditions + Genus													
II-Genus	494	2.49	0.72	0.55	310	4,374	5,438	14.8	0.0001*	-13.55	0.64	-21.17	<.0001*

1243

Table 8. Constant of fitted regression model explaining the $\delta^{13}C$ variability by morpho-functional groups. Model information includes value of the constant a ($\delta^{13}C$, ‰), standard error (SE), t ratio and Prob > |t|. Only morpho-functional groups with significant effects are enlisted.

Term	Estimated	SE	Razón t	Prob > |t|
Model constant	-14.2	0.4	-40.80	<.0001**
R-Smaller-sized articulated corallines	4.5	1.7	2.58	0.0100*
O-Compressed with branched or divided thallus	1.2	0.5	2.66	0.0079*
C-Erect thallus	1.8	0.6	2.84	0.0046*
R-Larger-sized articulated corallines	6.3	0.8	7.95	<.0001*
O-Hollow with spherical or subspherical shape	5.0	0.5	10.51	<.0001*
R-Blade-like with one of few layers of cells	-5.9	3.0	-1.98	0.0476*
C-Tubular	-1.6	0.5	-3.26	0.0012**
R-Filamentous uni&pluriseriate with erect thallus	-2.2	0.6	-3.92	<.0001*
R-Flattened macrophytes with cortication	-8.9	1.3	-7.10	<.0001*

*p<0.05, **p<0.0001

Table 9. Constant of fitted regression model explaining the $\delta^{13}C$ variability by genus. Model information includes value of the constant a ($\delta^{13}C$, ‰), standard error (SE), t ratio and Prob > |t|. Only genus with significant effects are enlisted.

Term	Estimated	SE	Razón t	Prob > |t|
Model constant	-14.7	0.2	-62.64	<.0001**
Corallina	6.4	2.9	2.22	0.0269*
Tacanoosca	3.5	1.3	2.71	0.0070*
Jania	5.0	1.7	2.97	0.0031*
Struveopsis	4.1	1.3	3.15	0.0017*
Codium	2.3	0.6	4.08	<.0001**
Padina	2.2	0.5	4.8	<.0001**
Hydroclathrus	7.3	1.1	6.59	<.0001**
Amphiroa	6.8	0.8	9.05	<.0001**
Colpomenia	5.4	0.4	14.02	<.0001*
Spyridia	-1.5	0.7	-2.10	0.0361*
Gracilaria	-0.9	0.4	-2.18	0.0294*
Polysiphonia	-3.7	0.8	-4.82	<.0001**
Schizymenia	-19.1	2.1	-9.33	<.0001**

*p<0.05, **p<0.001

Table 10. Constant of fitted regression model explaining the $\delta^{13}C$ variability by species. Model information includes value of the constant a ($\delta^{13}C$, ‰), standard error (SE), t ratio and Prob > |t|. Only genus with significant effects are enlisted.

Term	$\delta^{13}C$, ‰ estimated	SE	Razón t	Prob > |t|
Model constant	-14.6	0.2	-93.22	<.0001**
Hypnea pannosa	2.8	1.3	2.24	0.0256*
Colpomenia ramosa	3.2	1.4	2.27	0.0237*
Corallina vancouverensis	6.3	2.8	2.27	0.0238*
Caulerpa peltata	3.9	1.6	2.4	0.0165*
Codium sp.	3.0	1.3	2.4	0.0167*
Amphiroa misakiensis	7.1	2.8	2.55	0.0110*
Jania sp.	5.0	2.0	2.56	0.0106*
Codium brandegeei	2.8	1.1	2.63	0.0088**
Hypnea johnstonii	3.4	1.3	2.74	0.0063**
Tacanoosca uncinata	3.4	1.3	2.74	0.0062**
Struveopsis sp.	4.0	1.4	2.86	0.0044**
Padina durvillaei	1.4	0.5	2.87	0.0043**
Amphiroa sp.*3*	8.2	2.8	2.95	0.0033**
Codium simulans	3.2	0.9	3.41	0.0007**
Amphiroa sp.2	6.6	1.6	4.1	<.0001**
Colpomenia sinuosa	4.4	1.1	4.17	<.0001**

Colpomenia sp.	3.6	0.9	4.27	<.0001**
Padina sp.	3.5	0.7	4.77	<.0001**
Hydroclathrus clathratus	7.2	1.1	6.82	<.0001**
Amphiroa sp.	8.1	0.9	8.67	<.0001**
Colpomenia tuberculata	5.9	0.4	15.45	<.0001**
Spyrida sp.	-2.5	1.3	-1.97	0.0496*
Pyropia thuretii	-5.5	2.8	-1.98	0.0480*
Ulva acanthophora	-1.2	0.6	-2.06	0.0399*
Grateloupia filicina	-2.4	1.1	-2.08	0.0382*
Rhodymenia sp.	-4.1	2.0	-2.08	0.0380*
Ulva compressa	-3.2	1.4	-2.33	0.0203*
Rhizoclonium riparium	-5.1	1.6	-3.15	0.0017**
Polysiphonia sp.	-4.8	1.4	-3.44	0.0006**
Halymenia actinophysa	-9.9	2.8	-3.57	0.0004**
Cladophora microcladioides	-7.2	2.0	-3.64	0.0003**
Polysiphonia mollis	-5.2	1.1	-4.93	<.0001**
Schizymenia pacifica	-19.2	2.0	-9.76	<.0001**

*p<0.05, **p<0.001

1267 SUPLEMENTARY INFORMATION

1268

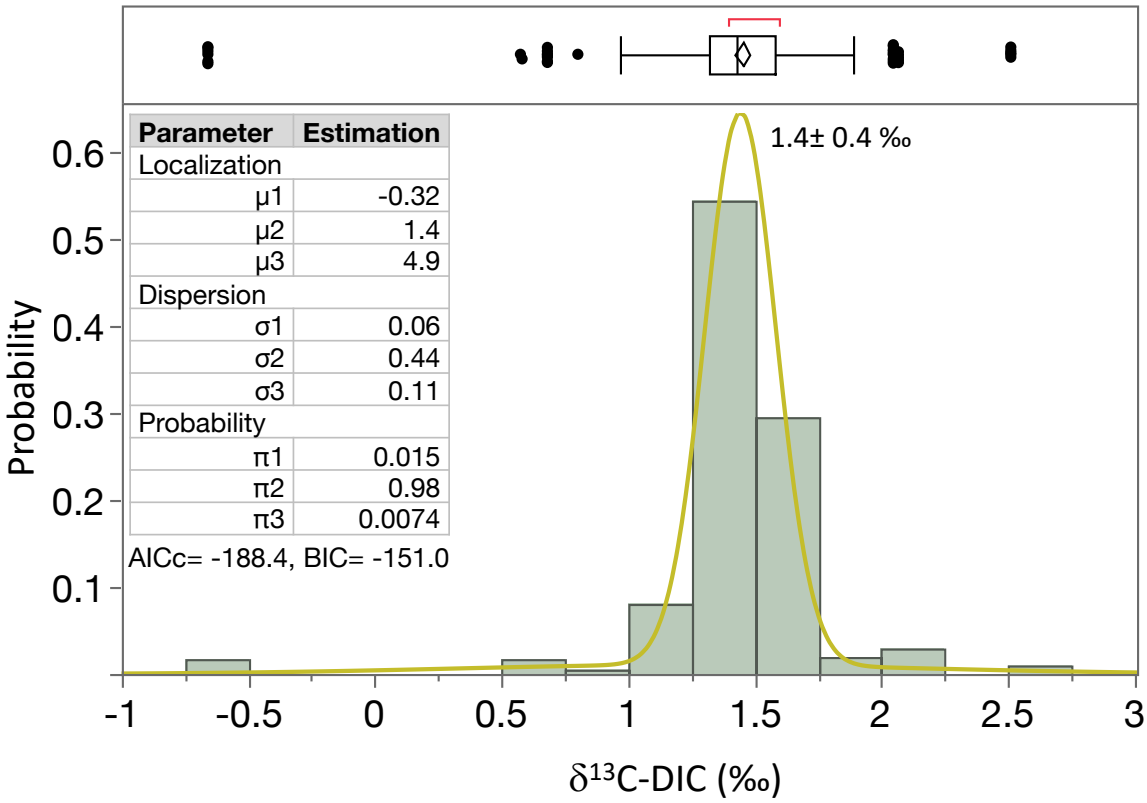

1269

1270 Fig. S1. Histogram representing the distribution of δ^{13}C-DIC values in surface seawater in the Gulf

1271 of California.

1272

1273

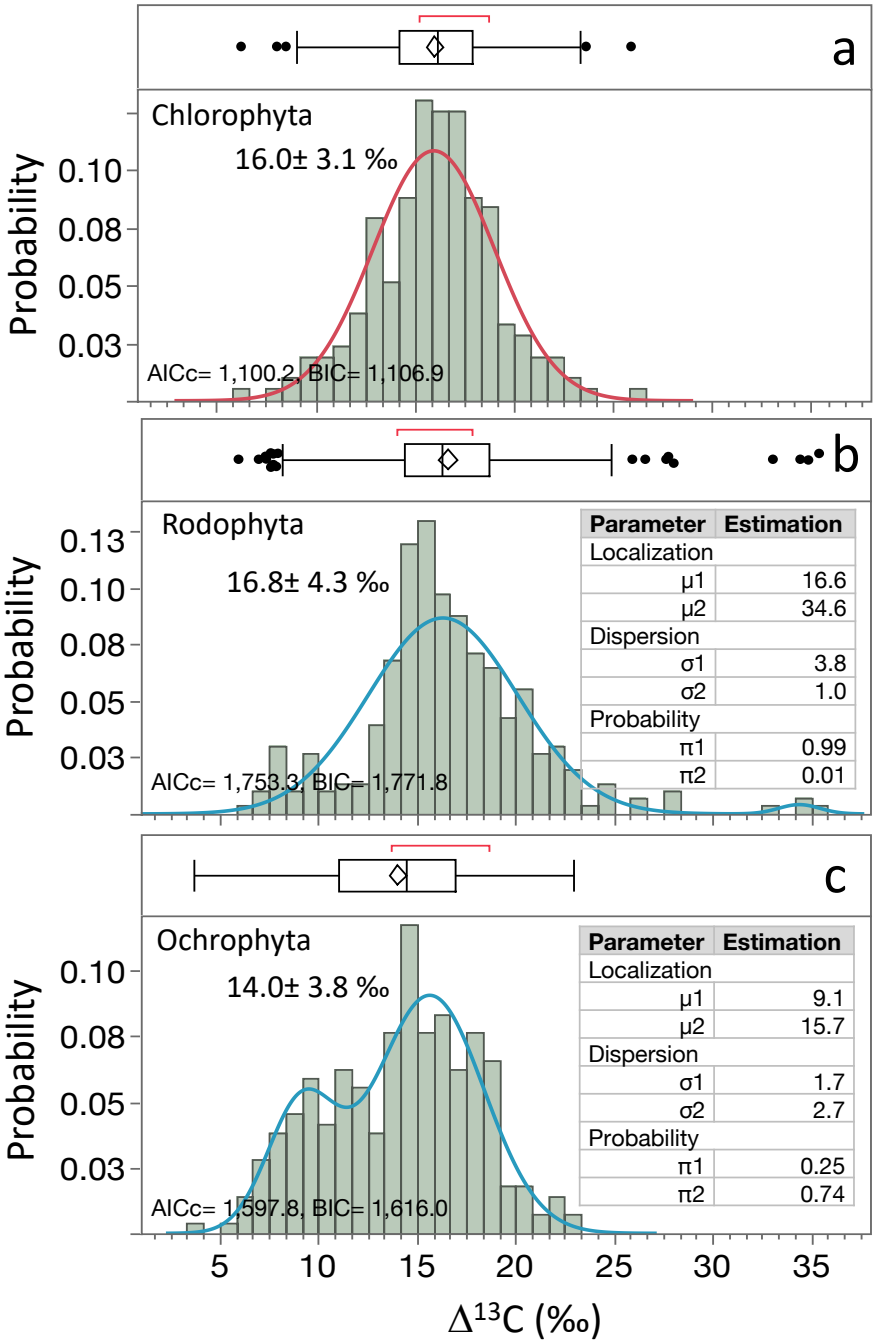

1274

1275 Fig. S2. Histograms representing the distribution of Δ^{13}C-macroalgal in macroalgae collected in the

1276 Gulf of California for Phyla a) Chlorophyta, Rhodophyta, and Ochrophyta.

1277